

RECOGNITION AND CLASSIFICATION OF GALAXIES WITH OPTICAL JETS

WILLIAM C. KEEL^{a)}Kitt Peak National Observatory, National Optical Astronomy Observatories,^{b)} P.O. Box 26732, Tucson, Arizona 85726-6732

Received 5 July 1985; revised 6 August 1985

ABSTRACT

Deep images and spectra are presented for galaxies reported in various catalogs to have jets, as well as in a search of the SRC J survey plates in a region near the south galactic pole. Most of these are shown to be superpositions, polar rings, tidal features, or artifacts of the original plate material. Examples are shown of ten ways that false jets can be produced, with more detailed case studies for several systems. Based on this experience, several criteria for the brightness, location, and symmetry of genuine optical jets are suggested, which should yield survey samples much less contaminated by "false alarms" than existing ones. Among the objects that remain as optical-jet candidates, ESO 0610-23 shows a linear, radial chain of H II regions on the outskirts of an amorphous system with complex internal structure, UGC 3995 is a close pair of spirals, one of which has a type 2 Seyfert nucleus and apparent knotty jet, and NGC 1598 has the radial features previously reported, but considerable chaotic outer structure as well. Several systems (such as AM 0207-49 and ESO 2330-38) illustrate the intrinsic difficulty of separating jets and tidal tails on morphological grounds alone in certain cases.

I. INTRODUCTION

Jets of ejected matter occupy an increasingly important place in the study of active galactic nuclei. They provide information on collimation, stability, and mass motion originating on very small scales compared to those of the jets themselves. To date, optical data on jets have been overshadowed by the radio observations. This is due in part to the relative ease of detection of these features with the VLA and their low level of optical emission, but sufficient additional insight could result from optical observations to justify considerable effort. Detection of emission lines would allow direct measurement of (projected) velocities associated with a jet (though not necessarily of the jet itself), and give information on the ionization mechanism and source of the gas. For continuum features, the long baseline from optical ($\approx 10^{14}$ Hz) to radio ($\approx 5 \times 10^9$ Hz) allows accurate determination of spectral shape and the location of such features as synchrotron breaks.

In several radio galaxies, some of this promise has been realized. The jet of M87 has no emission lines to very low limits (Sulentic, Arp, and Lorre 1979; Keel 1984), but the spectrum is well enough measured to locate an apparent synchrotron break. The optical and radio structures are, as nearly as can be determined, identical (Biretta, Owen, and Hardee 1983, Niéto and Lelièvre 1982), suggesting that external factors such as magnetic field geometry are dominant in producing the observed structure. Knots of optical emission coincident with radio features have been observed in NGC 7385 (Simkin and Ekers 1979; Simkin, Bicknell, and Bosma 1984) and in several 3C radio galaxies (e.g., Miley *et al.* 1981). Both continuum and line emission are seen; modest relative velocities are measured (≈ 500 km s⁻¹), perhaps suggesting entrainment of gas or interaction with the host galaxy's interstellar medium.

Going beyond the obvious jets of many radio galaxies, there is reason to suspect the existence of a population of

radio-quiet jets. The jets around the barred spiral NGC 1097 (e.g., Lorre 1978) are radio quiet to very low flux limits (Wolstencroft, Tully, and Perley 1984). Possible analogous features have been reported in NGC 1598 by Hawarden *et al.* (1979), while emission-line jets are found in at least two Seyfert galaxies. The possibility of another kind of ejection, seen mostly in spirals and leading to jets of different character than found in radio galaxies, prompted this investigation.

Several existing galaxy catalogs remark on the presence of jet-like features seen, for example, on Palomar Sky Survey plates. Many of these have been examined here in detail, and clues to their physical nature were sought. Many seem to be false alarms—superpositions of galaxies or stars, tidal tails, polar rings, or photographic artifacts—while a few may, in fact, represent matter ejected from galactic nuclei. The strongest result of this study is that very few of the galaxies observed seem to have actual jets; most of the ones so far noted in catalogs are other kinds of phenomena.

II. GALAXY SELECTION AND OBSERVATIONS

a) Galaxies from the Literature

All objects listed as having jets in the Uppsala (Nilson 1973) and ESO (Lauberts 1982) catalogs, the Zwicky (1971) catalog of compact and posteruptive galaxies, and Michigan-Tololo emission-line surveys (MacAlpine, Lewis, and Smith 1977; MacAlpine and Lewis 1978) were inspected on Palomar, ESO B, or SRC J survey plate glass copies to assess the nature of each feature reported. A number were obvious tidal features (based on the criteria discussed in Sec. IIIb, which were formulated early in the study) or not clearly present, and not examined further. Additional objects were taken from the Arp (1966) Atlas (such as VV 144) and from papers already cited for NGC 1097 and 1598. The whole list of candidates appears in Table I, along with a summary of the observations obtained for each Sec. IIc,d).

b) South Galactic Pole Sample

To supplement the objects selected above, four fields of the SRC J survey were examined closely for galaxies with features resembling jets. This material is especially suitable for such use because it has a lower limiting surface brightness

^{a)} Visiting Astronomer, Cerro Tololo Inter-American Observatory, National Optical Astronomy Observatories. Present address: Sterrewacht Leiden, Postbus 9513, 2300 RA Leiden, The Netherlands.

^{b)} Operated by the Association of Universities for Research in Astronomy, Inc., under contract with the National Science Foundation.

TABLE I. Observations of suspected jet galaxies.

Object	Jet type	α	δ	Images	Spectra		cz (km/s)	Notes
					Nucleus	Jet		
NGC 1097	Jets	02 44 11.0	-30 29 00	CTIO CCD	SIT	SIT	1227	
PKS 0521-36	Jet	05 21 12.9	-36 30 17	CTIO CCD	SIT	SIT	16590	2cm, 6cm
NGC 1598	?	04 27 08	-47 53 24	CTIO CCD			5126	
NGC 2534	Not found	08 08 58.7	+55 49 20	KPNO IT	IIDS		3710	
M87	Jet	12 28 17.5	+12 40 02	2.1-m CCD	CCD	CCD	1254	
II Zw 23	Accreting?	04 47 07.0	+03 14 55	KPNO CCD	CCD	CCD	8320	20cm
I Zw 96	Tidal	14 43 14.8	+51 33 03	KPNO CCD	CCD	CCD	26830	20cm
VV144	Tidal	11 29 48.0	+54 39 24	VCAM	CCD	CCD	6200	20cm
NGC 3303B	Tidal?	10 34 17.9	+18 23 48	2.1-m CCD	CCD	CCD	5968	20cm; A at cz=6015
IC 883	Tidal	13 18 17.5	+34 23 58	2.1-m CCD	CCD	CCD	6885	
NGC 7135	Merger	21 46 48	-35 07 00	PSS	IDS		2050	LINER nucleus; broad H α ?
NGC 1602	H II chain	04 26 48	-55 10 00	CTIO CCD	SIT	SIT	1740	
AM 0206-49	Tidal	02 06 58	-49 32 00	CTIO CCD	SIT	SIT	17500	Sy 2+companion at cz=17230
UGC 262	Tidal	00 24 36	+39 31 00	KPNO IT			IV Zw 20
UGC 360	Not present	00 33 40.7	+25 31 56	KPNO CCD	CCD	(CCD)	9760	Faint tidal features
UGC 573	Edge-on spiral	00 53 24	+13 57 00	KPNO IT			NGC 304, IV Zw 34
UGC 1078	"Stems"	01 27 54.0	+41 00 00	VCAM+IT		IDS	1745	NGC 573
UGC 1378	Not present	01 51 59.9	+73 02 19	KPNO CCD	CCD	(CCD)	2930	
UGC 1488	Oblique ring	01 57 42	+27 59 00	KPNO IT			NGC 780, V Zw 164
UGC 2792	Not present	03 32 24	+72 24 00	PSS	CCD	(CCD)	2180	H II ring around nucleus
UGC 3031/2	Tidal	04 21 48	-00 51 00	KPNO IT			NGC 1568ab, II Zw 10
UGC 3071	Int. spiral	04 28 30	+07 31 00	KPNO IT			NGC 1590, II Zw 13
UGC 3810	Superposition	07 18 06	+46 56 00	KPNO IT			
UGC 3890	Not present	07 28 00	+83 54 00	KPNO IT			
UGC 3995	Jet?	07 41 01.7	+29 22 04	VCAM+IT	IIDS		4960	20cm; Sy 2+companion at cz=4560
UGC 4261	?	08 07 40.2	+36 58 39	PSS	IDS		5466	H II nucleus
UGC 4556	Tidal	08 40 56.1	+41 54 07	PSS	IDS		1060	H II nucleus; like VV144
UGC 5050	Edge-on	09 25 44.4	+76 41 03	Arp atlas	CCD	CCD	2290	
UGC 5101	Tidal	09 32 04.6	+61 34 37	PSS	IIDS		11945	Like IC 1182; reddened active nucleus
UGC 6435	Not present	11 23 01.4	-00 29 35	KPNO CCD	CCD	(CCD)	7620	
UGC 9621 comp	—	14 55 00	+82 45 00	PSS			
UGC 10857b	Tidal	17 24 56.1	+53 34 43	2.1-m CCD	IDS		8550	H II nucleus; A at cz=8780
UGC 11916	Complex str.	22 05 58.2	+18 12 30	VCAM	IIDS		1530	II Zw 166
UGC 12552 comp	Tidal	23 20 37.58	+12 46 17	VCAM			III Zw 104
ESO 0058-58	Blobs	00 58 28	-58 01 12	CTIO CCD	SIT	SIT	3130	
ESO 0304-47	Int. gal.	03 04 31	-47 02 24	CTIO CCD	SIT	SIT	18190	
ESO 0534-52	Superposition	05 34 38	-52 10 24	CTIO CCD				
ESO 0610-23	Jet? H II	06 10 04	-23 31 30	CTIO CCD	IDS	SIT	1760	20cm
ESO 2138-46	Polar ring	21 38 45	-46 14 18	CTIO CCD	SIT	SIT	17700	
ESO 2330-38	Tidal	23 30 49	-38 52 24	CTIO CCD	SIT	SIT	9750	
UM 221	Star/gal.	00 12 10	-00 16 24	CTIO CCD				
UM 254	Int. gal.	00 29 00	-02 26 00	CTIO CCD				
UM 345	Int. gal.	01 34 37	+00 37 42	CTIO CCD				
UM 384	Star/gal.	01 56 35	+00 50 48	CTIO CCD				

Notes to Table 1:

All positions are for 1950 and the most accurate available. Most were measured on glass copies of the Palomar or ESO/SRC surveys. Those with obvious rounding are from the ESO or UGC catalogs.

Images: KPNO IT=KPNO 2.1-m with Carnegie image tube, B or R filter, 10-m exposure. KPNO CCD=KPNO 4-m with Cryogenic Camera, TI CCD, B or R. CTIO CCD=CTIO 4-m with RCA CCD at prime focus, B and V. 2.1-m CCD=KPNO 2.1-m with TI CCD at $f/7.5$, B,V,R. PSS: glass copies of Palomar or SRC sky survey plates.

Spectra: CCD=KPNO 4-m with Cryogenic Camera; redshifts accurate to 50 km/s. SIT=CTIO 4-m with SIT-Vidicon; redshifts accuracy 200 km/s. IIDS=KPNO 2.1-m with Intensified Image-Dissector Scanner; accuracy 100 km/s. IDS=Mt. Lemmon 1.5-m with Image-Dissector Scanner; accuracy 150 km/s. All new redshifts are heliocentric. Parentheses indicate that a feature is either not present or was not detected.

than the Palomar survey. Eight objects were found, listed in Table II and denoted by the prefix SGP, of which five proved to be nonexistent on deep CCD images and two are probably tidal in nature. With improvements in search criteria based on these results, this survey has been extended to the entire southern sky ($\delta < -18^\circ$ and $|b| \geq 15^\circ$), with results to be presented elsewhere.

c) Images

The galaxies in this program have been imaged with a variety of instruments, identified in Tables I and II. Four-

teen UGC and Zwicky objects were photographed with the KPNO 2.1 m telescope, Carnegie image tube, and filters approximating *B* and *R* in November 1982; 10 min exposures with these broadband filters were long enough to be sky limited (background density about 1.5). Images of UGC 360, UGC 1378, II Zw 23, and I Zw 96 were obtained with the KPNO 4 m and Cryogenic Camera CCD in direct mode (0.86 arcsec per pixel, 5' field) in December 1982. Broadband images (and in some cases H α as well) were obtained of III Zw 104, UGC 3995, UGC 11916, NGC 3303, and NGC 573 with the video camera (ISIT) at the KPNO 2.1 m telescope. Additional broadband images, of M87, NGC 3303, UGC

TABLE II. Jet candidates in the south galactic pole region.

Object	Type of jet	α (1950) δ		cz (km/s)
SGP 1	Polar ring	23 49.1	- 39 26	19 540
SGP 2	Interacting gal.	23 57.4	- 37 02	41 400
SGP 4	Jet?	00 20.5	- 39 59	12 500
SGP 5	Not present	00 14.9	- 39 47	—
SGP 7	Not present	23 43.7	- 37 01	—
SGP 8	Not present	23 50.8	- 37 28	—

10857B, and IC 883, were obtained with the 2.1 m and an 800 \times 800 TI CCD.

Most of the images were obtained using an RCA CCD at the prime focus of the Cerro Tololo 4 m in September 1983. The field was 3.7 \times 5.0 arcmin, at 0.59 arcsec per pixel. Seeing was usually near 1.5 arcsec FWHM. Images in *B* and *V* were obtained, with photometric calibration possible through observations of the E-region standards of Graham (1982). The RCA chip gives interference fringes in the *V* band, due to night-sky [O I] λ 5577 emission. These fringes were removed from the flat-fielded frames by subtraction of a standard "library" fringe pattern, using an interactively determined scale factor for each frame. This procedure usually removed the fringing to a level below 1% of the night-sky level. Measures of the galaxy and jet magnitudes were possible with some precision, and will be discussed where relevant. The images themselves will be presented and discussed for various classes of objects in later sections.

d) Spectroscopy

Spectra of most of the galactic nuclei, and a few of the jets, in the present sample have been obtained with a similar variety of detectors. Aperture spectrophotometry was performed with the 1.5 m UCSD-UM reflector on Mount Lemmon and the KPNO 2.1 m, using basically similar image-dissector scanner systems over the range 3700–7000 Å; 4.7 and 6.1 arcsec apertures were used, respectively.

The Cryogenic Camera was used in both long-slit and aperture-plate spectroscopic modes. The range 4400–8000 Å was covered at a resolution near 20 Å (resolutions are quoted as full width at half-maximum). Frequent calibration data and the stability of this system mean that the wavelength scale is reliable to about 30 km/s, and the relative photometric scale to a few percent. The slit width was 2.5", projecting to about 3 pixels at 0.86" per pixel spatially and about 4 Å spectrally. Aperture-plate data used 2.5" circular holes drilled to observe nuclei, "jets," and tails simultaneously. Data of this type for IC 883 and NGC 3303 are reported here. The positions to be observed were identified and measured on 5 m plates taken by Arp, who kindly allowed their use for this purpose. The reduction procedures are described elsewhere (Keel 1985a), while the observed positions and spectra are shown in Sec. IIIb.

Further slit spectra were obtained with the SIT-Vidicon "Big UV" system at the RC spectrograph of the CTIO 4 m. The range observed was 4100–7100 Å, with resolution near 6 Å. A format of 1400 spectral by 180 spatial pixels (180 arcsec) was used. Instabilities in the detector were serious during this run; observing and reduction procedures were selected to reduce their effects. Bias-pattern frames were taken hourly and subtracted from the raw data to account partially for temporal changes in the bias level and structure; further correction employed smoothed blank-sky spectra (after sky

subtraction), which contained effects of drift during each exposure and were subtracted from the galaxy spectra. Some residual interference patterns generally remained toward the red end of each spectrum; for such purposes as H α velocity curves, the dominant interfering spatial frequency was removed in the Fourier domain, and measurements performed after transforming back to the observed spatial and spectral domain.

All long-slit spectra were reduced with the *RV* routines of the IPPS, in which data are rebinned in each direction to place each frame on a linear wavelength scale and a spatial system which is in register at each wavelength. Observations of Stone (1974, 1977) standard stars were used to place the spectra on relative flux (F_λ) scales, allowing estimates of various line ratios and continuum-shape parameters. Comparison of elliptical galaxy flux distributions known from large-aperture IDS data indicate that the Cryogenic Camera data are photometrically accurate shortward of 7500 Å, beyond which defocusing at the chip is important; the SIT data are photometrically useful from 4500 to 6000 Å for sources well above the dark-current plus readout-pattern level and below saturation.

These spectra were used to derive redshifts and nuclear properties for the program galaxies, as given in Tables I and II. In a few cases, spectra of the jets themselves (or apparent jets) were obtained. Results for M87, VV 144, and I Zw 96 have appeared elsewhere (Keel 1984, 1985a); others are discussed in more detail below.

e) Radio Continuum Mapping

Several of the more interesting systems in Table I were mapped with the VLA* in January 1984, to see whether any of the apparent jets contain synchrotron-emitting material such as is characteristic of radio-selected jets. UGC 3995, ESO 0610-23, NGC 3303, and III Zw 104 were observed, as well as VV 144, I Zw 96, and II Zw 23 (for which results are reported elsewhere; Keel 1985a,d). The standard B array was employed at 20 cm, with 50 MHz bandwidth. Total integration times of 40–56 min were used.

The limiting flux level reached was about 0.3 mJy per beam (4" diameter). None of the jets were detected; the nuclei of VV 144 and UGC 3995 were detected at 1.59 and 7.8 mJy, respectively (1514 MHz). The nucleus of NGC 3303A was detected at about 2 mJy; confusing sources nearby limit accurate measures for this object. Extended structure is present in II Zw 23, but seems to reflect the propagation of star formation in a nonequilibrium envelope rather than motions governed by nuclear activity (Keel 1985d).

III. TEN WAYS TO MIMIC AN OPTICAL JET

These results show the effects of at least ten ways of faking the appearance of an optical jet. Some are obvious, but are included here for completeness and illustration. The figures form to some extent an atlas of the kinds of images that can appear jet-like, but have convincing and more prosaic explanations.

a) Galaxy Superpositions

Some jets turn out to be chance alignments of galaxies, for example an edge-on spiral aligned with the nucleus of an

*The Very Large Array is a facility of the National Radio Astronomy Observatory, which is operated by Associated Universities, Inc., under contract with the National Science Foundation.

other galaxy. This seems to be the case in the radio source DA 240 (van Breugel *et al.* 1983) and in 1240-057 (Romaniushin 1984). Two more, UGC 3810 and ESO 0534-52, are shown in Fig. 1 [Plate 215]. Both are relatively convincing at the depth and scale of Sky Survey plates. Situations such as these are bound to arise in any optical search, in numbers governed by the parameters (magnitude range, narrowness, and alignment criteria) of such a search.

b) Tidal Effects and Interacting Galaxies

This group, in principle, overlaps *a*, but the main emphasis here is on tails drawn out of a galaxy which may appear quite straight and narrow in projection; visual searches select strongly in favor of such objects. The cases of VV 144 and I Zw 96 have been examined in detail (Keel 1985a); VV 144 shows direct dynamical evidence of resulting from a slow encounter between elliptical and disk galaxies, and there is strong circumstantial evidence in I Zw 96. Some further examples from this survey appear in Fig. 2 [Plate 216].

Segregation of tidal and nuclear effects in interacting galaxies requires some care. Ignoring interacting galaxies altogether will lead to exclusion of many objects with active nuclei and thus clear potential for jets, since nuclear activity is enhanced in interacting systems, and radio jets with internal signs of interaction are seen in multiple galaxies (e.g., 3C 75, Owen *et al.* 1985). Direct evidence of stars in a continuous and moderate velocity field, as was possible in VV 144, is compelling, particularly when predictions of tidal models (e.g., Toomre and Toomre 1972; Quinn 1984) may be applied and are consistent with both the morphology and dynamics.

For less ordinary features such as chains of H II regions, the separation is less clear, even in principle. Interactions, advanced to the stage of mergers, can produce a menagerie of effects when gas-rich systems are involved, and selecting for radial structures will undoubtedly produce some fraction of these. Either dynamical or circumstantial arguments based on the level of nuclear activity now observed might be adduced in interpreting such a feature.

On purely morphological grounds, certain kinds of tidal features can be recognized. Systems such as NGC 1568 [Fig. 2(a)], with nearly symmetric pairs of tails, are not likely to appear as jets on images with sufficient resolution. One-sided features such as that of IV Zw 120 [Fig. 2(b)] are more diffi-

cult to interpret without further data. In this instance, the width of the feature, slight curvature, and terminating bend are more characteristic of tidal features than of jets.

Disruption of dwarf companion galaxies can produce particularly narrow structures. The jet of M89 (Malin 1979; Malin and Murdin 1984) now appears, from the galaxy's shells and the detection of stars in the jet, to be the remnant of such a process. In the present sample, ESO 2330-38 may represent an analog involving a disk galaxy, perhaps about to produce a polar ring. This object [Fig. 2(c)] has a faint plume (integrated $V = 17.29$, $B - V = 0.32$) nearly at right angles in projection to the disk of the main galaxy. A SIT spectrum along the galaxy's major axis shows a number of luminous H II regions in ordered motion suggestive of rotation, with the north side approaching; the velocity range covered is about 800 km/s, which is unusual for a galaxy of this luminosity ($M_V \approx -21$, depending on the amount of internal obscuration); the large velocity spread may indicate dynamical disturbance associated with a strong interaction, which could produce ordered but not purely rotational motions. Another spectrum along the plume, through the nucleus of the main galaxy, shows no emission lines in the plume, so that its light is not dominated by emission; at this surface brightness, no continuum detection would be expected with the SIT. However, extended [O III] λ 5007 emission (and perhaps H β) appears on the *other* side of the nucleus [Fig. 3(a)]. This presumably reflects matter disturbed by the production of the plume; since it extends all the way into the galaxy, the emission might arise in a part of it wrapped around the galactic nucleus. It is tempting to speculate that after a few orbital periods this object will have a nearly symmetric polar ring. The absolute magnitude ($M_V \approx -17.6$) and color of the plume are consistent with its being the remnant of a dwarf irregular galaxy such as the SMC. Arguments against this being matter ejected from the nucleus include the fact that it does not trace back to the nucleus but is misaligned by 4" (2 kpc), and the lack of strong activity other than star formation as shown in the nuclear spectrum [Fig. 3(b)]. The structure of the galaxy shows dust lanes crossing the plane near the nucleus on each side; the parts of the inner region visible between the lanes may be the discrete "nuclear condensations" mentioned by Sol (1983). The [N II] λ 6584/H α ratio shows a distinct maximum at the continuum peak position, suggesting that this is coincident with the genuine nucleus,

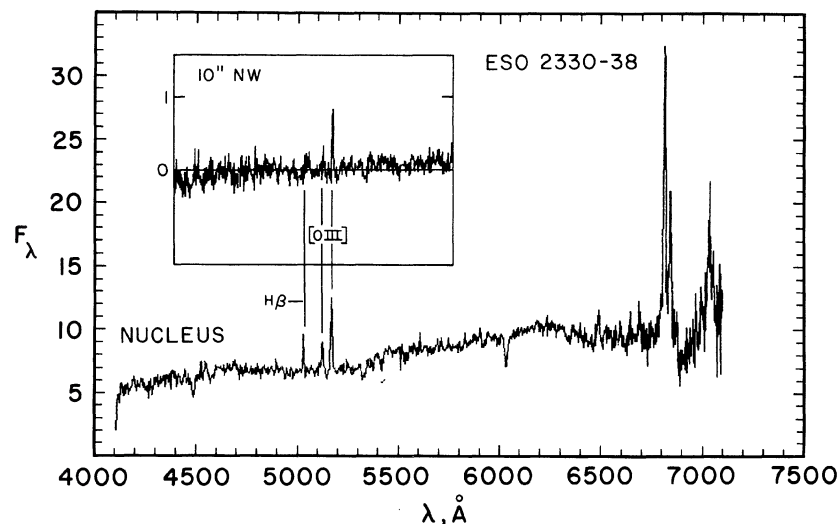


FIG. 3. CTIO SIT spectra of ESO 2330-38, from the sum of three 10 min exposures. Inset, a region opposite the plume, 10–15" NW of the nucleus in P.A. 104°. [O III] λ 5007 appears, probably accompanied by H β ; no corresponding continuum extension is seen in images. Large panel, the nuclear spectrum, showing emission lines dominated by effects of current star formation; a LINER contribution is present, seen in the high [N II]/H α ratio and its distinct peak at the nucleus.

while the other emission-line features are surrounding H II regions. The presence of LINER-like spectral features at the very nucleus indicates the presence of weak, but not dominant, nonstellar activity; this level of activity is rather common among luminous disk systems.

Mergers can produce even more striking plumes and tails than are seen in interactions between well-separated galaxies. Again, velocity fields and stellar populations can indicate that some features are results of mergers. The tails of IC 883, for example, were illustrated by Arp (1966) as possible jets. The system shows both a narrow jet and a broader, more diffuse tail, with three central condensations. Two of these condensations, four positions in the jet, and two in the tail, were observed spectroscopically with the Cryogenic Camera (Fig. 4, [Plate 217]). The spectra so obtained show a composite stellar continuum, with nuclear emission lines mostly produced through stellar photoionization (Fig. 5). One of the nuclei shows strong [O I] λ 6300 and may therefore have significant energy input to the gas from shocks, as seems likely in a merging system, or from a weak power-law UV source. The relative velocities in this system are large, with mean radial velocities from the features measured of 6680 ± 100 km/s in A and 7100 ± 50 in B. An average of the four jet positions [Fig. 5(d)] shows H β in absorption at 7380 ± 100 km/s. The equivalent width of H β here, 9 \AA , is not unusual for a stellar population of this color and continuum shape, so that the features in IC 883 are probably tidal in origin.

Similar observations of NGC 3303 A-B were obtained, with less conclusive results. This system contains an elliptical and a barred spiral, from which issues a narrow, slightly curved feature (Fig. 6, [Plate 218]). Spectra of this jet, the galaxy nuclei, and various structures in both galaxies were obtained with the Cryogenic Camera aperture-plate system. Both nuclei have strong low-ionization emission lines [Figs. 7(a),(b)]. Nothing remarkable appears at the jet position; there is certainly no obvious emission-line enhancement [Fig. 7(c)]. There is thus no evidence for nonstellar processes

in the jet, though nontrivial amounts of continuum emission could be present—up to 20% from absorption-line equivalent widths and filling-in limits. It is worth noting that the level of emission-line activity in the elliptical NGC 3303A is very high for an elliptical galaxy, comparable to that seen in NGC 1052; however, this object is a weak emitter in the radio (Sec. IIe), making it considerably less luminous than NGC 1052 at 20 cm.

There are several objects observed in this study that show features possibly due to interactions, but whose precise origin remains unclear. AM 0207-49 (Fig. 8(a), [Plate 219]) is a spiral galaxy plus companions in a linear arrangement, with extensive diffuse matter. The prominent stellar object along the chain is a foreground F star. This system was illustrated by Arp and Madore (1977) as one with an apparent jet. The nucleus of the spiral is a Type 2 Seyfert, somewhat unusual in the strength of [O I] λ 6300 and [N I] λ 5199 emission (Fig. 9). The companion galaxy immediately to the west shows H β and Mg I absorption at a radial velocity ~ 270 km/s less than that of the brightest galaxy. No emission lines were detected on a poorly exposed SIT spectrum of the knots at the extreme end of the plume. The tilt of the bright companion with respect to the plume, its offset with respect to the primary nucleus, and the “hook” at its outer end suggest this as an example of tidal distortion.

The case of ESO 0304-47 is somewhat similar [Fig. 8(b)]. The tail arises nearly tangent to the inner disk of the main galaxy, in the direction of the bright companion. A spectrum along this bridge was not well enough exposed to reveal absorption features; no emission lines appeared, indicating that it is predominantly a continuum feature. Such galaxies as these illustrate the morphological difficulty of classifying some of these systems without further information. As a further example, Bertola and Sharp (1984) have noted that the prominent chain of H II regions in NGC 3310 may be interpreted as well by a jet picture as by a merger, as suggested by Balick and Heckman (1981).

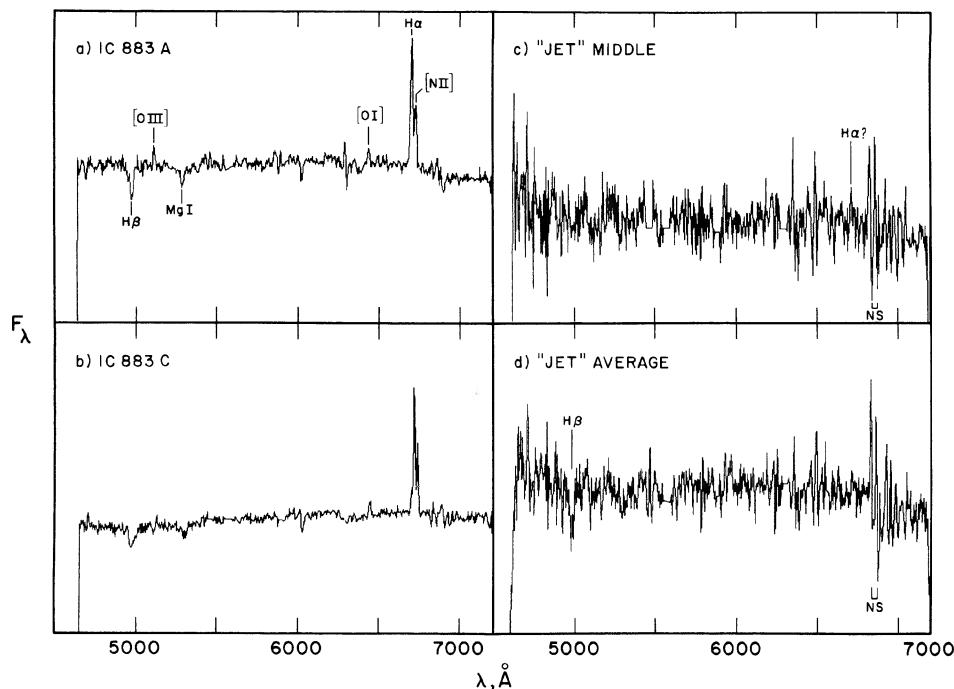


FIG. 5. Aperture-plate spectra of IC 883, from a total of 25 min exposure with the Cryogenic Camera at the KPNO 4 m. The scale is relative F_{λ} , with the zero-flux line at the bottom of each frame. (a) The brightest (southern) peak. The continuum indicates a strongly composite stellar population, with strong Balmer and Mg + MgH absorption. The strength of [O I] λ 6300 in (a) and (b) may indicate significant shock ionization. (b) A secondary (northern) peak, showing features similar to those in (a), with a slightly bluer continuum. These two regions differ by 400 km/s in radial velocity. (c) The second jet positions from the southeast end (Fig. 4), showing possible weak H α emission. (d) An average of the four jet positions observed. H β absorption is prominent, with indications of Mg + MgH near 5300 \AA . The strong features in the red are night-sky residuals.

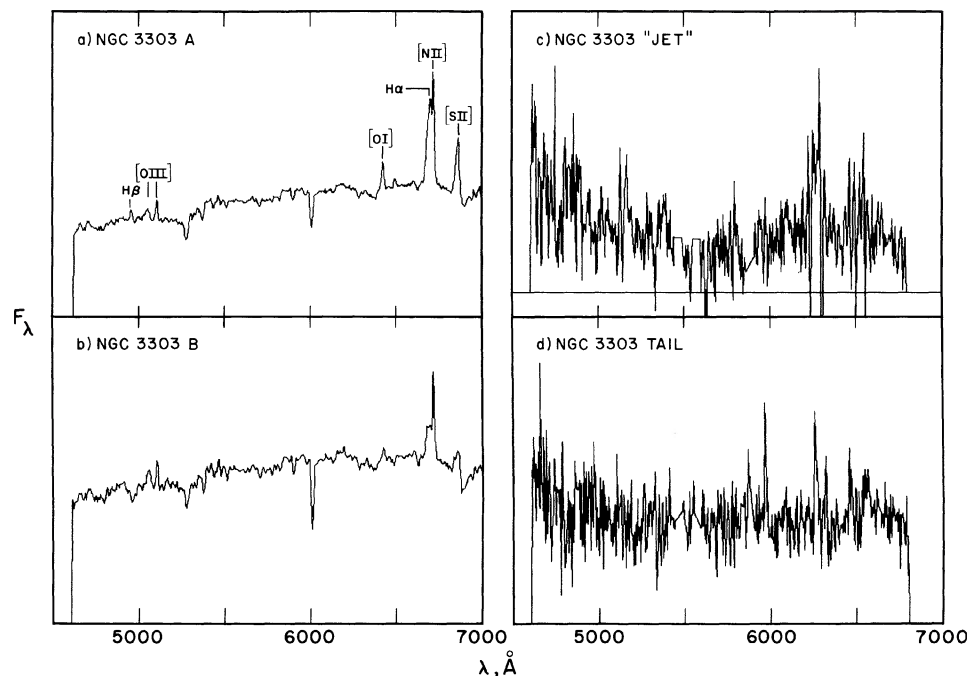


FIG. 7. Aperture-plate spectra of NGC 3303, obtained with 45 min exposure using the Cryogenic Camera. Spectra are shown on a relative F_λ scale; unless otherwise indicated, the zero level is at the bottom of each panel. (a) Nucleus of the elliptical galaxy (A), showing strong low-ionization emission and possible broad H α . (b) Nucleus of the barred spiral (B), showing weaker low-ionization emission with very high [N II]/H α . (c) Outer part of the apparent jet of NGC 3303; the feature near 6300 Å is a night-sky residual. (d) Outer region of the tail of NGC 3303; a blue continuum is apparent, but no spectral features are visible (peaks to the red are night-sky residuals).

c) Galaxies with Polar Rings

These systems are most easily detected when the main galaxy's disk is seen nearly edgewise (Schweizer, Whitmore, and Rubin 1983), and many of them also have outer (perpendicular) rings seen almost edge-on. The rings of NGC 4650A and UGC 7576 were in fact originally interpreted as pairs of jets (Laustsen and West 1980; Sofue *et al.* 1982; Mould *et al.* 1982). These may be distinguished from true jets in being very symmetric about the central body; the optical jets so far known are either one-sided or quite asymmetric (e.g., NGC 1097, for which Lorre 1978 reported brightness ratios of 9:1 and 3:1 for the opposing pairs of jets; this is the most symmetric case yet studied). When not quite edge-on, they frequently show absorption against the central galaxy.

Several polar rings and apparently related objects were observed. Images are shown in Fig. 10 [Plate 220]. SGP 1

(2349-394) shows luminous material in a broad band over the poles of the central lens. In ESO 2138-46 and NGC 780, two disk planes are seen, differing by 30°-40°; these may be "non-polar rings," which should have a much shorter lifetime and be correspondingly rarer than the perpendicular variety, following the dynamical arguments given by Schweizer, Whitmore, and Rubin (1983). The morphological clues to the presence of an outer, misaligned ring frequently require high-resolution images, so the distinction between rings and jets is often not apparent (except from symmetry considerations) from sky-survey plates.

d) Asymmetric Light Distributions in Edge-On Galaxies

It has long been recognized that the tendency of dust lanes to lie along the insides of spiral arms produces a strong asymmetry in the appearance of a spiral galaxy when viewed

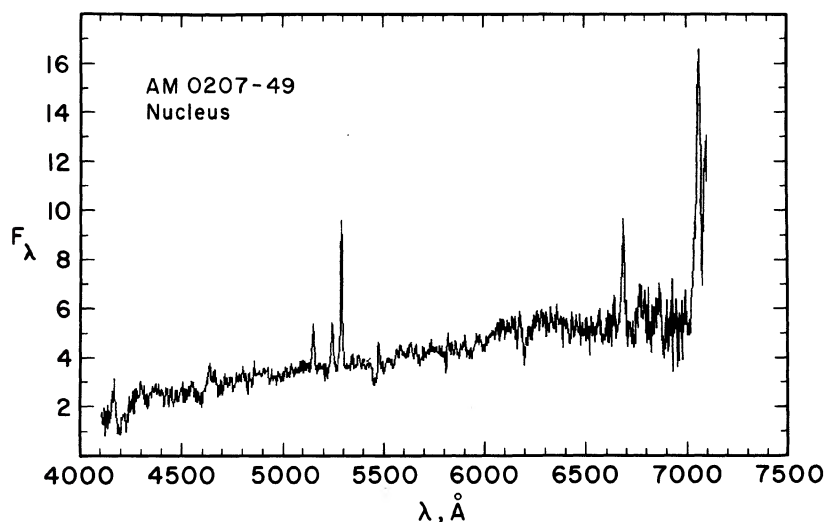


FIG. 9. SIT-Vidicon spectrum of the nucleus of AM 0207-49. The object is a Type 2 Seyfert, somewhat unusual in the strength of [N II] λ 6580 and [O I] λ 6300.

along its plane (Tsitsin 1955; de Vaucouleurs 1958). For a trailing spiral pattern, this means that the approaching side of the disk is brighter than the receding side. This contrast may be so extreme as to give the appearance of a jet along the major axis, as seen in UGC 5050 = Arp 207 (Fig. 11, [Plate 221]).

A spectrum in the region of $H\alpha$, along the major axis, is also illustrated in Fig. 11. The emission lines are spatially very clumpy and exhibit no obvious velocity ordering. This is a result of patchy extinction, whereby the inner parts of the image consist of light from the outer arms (with low differential velocities) and from inner-arm material seen through relatively clear regions (with higher differential velocities, since they may be seen near the apparent ends of their orbits). The spectrum of UGC 5050 may be understood in this way as the superposition of several solid-body-like projected rotation curves partially outlined by $H\ II$ regions. A nearly flat rotation curve for the galaxy means that the maximum velocity difference is not strongly dependent on projected distance from the nucleus, though a single direction of rotation means that two opposing quadrants of the position-velocity plane are "forbidden" (as in the study of our own galactic center). At least three arms (or emission-rich radial zones) may be identified in UGC 5050.

One of the objects from the SGP survey (0051.8-3745, not observed here) is clearly of this type, as are UGC 5485 and possibly IC 4697. These were found so often on sky-survey plates that it seems most fruitful to ignore any jet-like features along the major axis of a highly flattened galaxy, though this might result in missing some (small fraction of) true jets.

e) Galaxies with Optical Filament Systems

Several kinds of extensive (emission-line) filament systems are known to occur around galaxies, some of which have features that mimic the appearance of jets. A number of central cluster galaxies have emission-line filaments apparently associated with accretion flows (e.g., Heckman 1980). Such structures in M87 appear to have been the "counterjet" seen in emission lines by Arp (1967), based on the $H\alpha$ images obtained by Ford and Butcher (1979). Some of these features seen singly, especially those around NGC 1275, could well appear as jets.

Additional quasistationary or infalling filaments are seen in elliptical galaxies with associated "blue knots," such as NGC 3561 and IC 1182 (Stockton 1972). Stockton concluded that these are star-forming regions in an intergalactic medium. Among objects examined for this survey, II Zw 23 shows ~ 7 radial filaments with terminating knots. Spectroscopy suggests that the filaments are falling into the galaxy (Keel 1985d). These findings suggest that galaxies with too many jets or a filamentary appearance should be ruled out of optical-jet surveys.

f) Normal Galactic Bars

Occasionally, especially in the Zwicky catalog, objects are listed as jets that seem to be, on closer inspection, fairly ordinary bars in faint disks. An example is VII Zw 3 (Fig. 12, [Plate 222]). These galaxies may be eliminated from surveys by rejecting bright, symmetric pairs of features, as in the case of polar rings.

g) Galaxies with "Stems"

Vorontsov-Velyaminov (1959, 1977) has called attention to systems that show relatively short connections to outlying luminous patches. These may occur over a range in morphological type; some of the galaxies in *e* are included. When data are available, these features are found to be associated with active star formation, and could result from its propagation in an outer disk. As an example, the inner disk and outer parts of NGC 573 = UGC 1078 are shown in Fig. 13 [Plate 223]. The inner regions show clear spiral structure; an IDS spectrum shows nuclear emission lines indicative of star formation there. Because the stems do not reach far back toward the nucleus, they are more likely features of local rather than nuclear origin.

h) Superimposed Stars

When projected against the steep background of a galaxy halo and convolved with seeing, stars may produce effects quite like those of jets on certain isophotes. This can be particularly troublesome in view of the fact that some synchrotron jets are strongly dominated by relatively small regions that will appear stellar at redshifts greater than about 0.10. For example, the continuum object near Fairall 71 interpreted by Fricke, Kollatschny, and Loose (1984) as a synchrotron jet is stellar in appearance. The jet of M87 is sufficiently dominated by small regions (knots A, B, and C) that at a distance corresponding to $z \approx 0.05$ its jet would not be resolved from the ground.

Compact companion galaxies can produce effects quite like those of stars. The four Michigan-Tololo (UM) objects examined all seem to be interacting or double galaxies in which the companion was not well separated from the primary on Sky Survey plates (Fig. 14), or in two cases possibly foreground stars.

A jet can be simulated by superimposing a star or compact companion on the outer part of a galaxy image, especially in photographic searches in which only a limited intensity range is well exposed. These cases need to be examined individually in some detail before complete rejection; some objects such as F71 are probably missed in morphological surveys because of the large number of foreground stars compared to similar-appearing knots of ejected material appearing close to the galaxies.

Stellar diffraction spikes can also cause confusion on images taken with a single instrument. A star projected within the image of a galaxy can produce one to four jet-like structures, while a galaxy appearing along a diffraction spike, even at some distance, may show image structure due to enhanced exposure along the spike. In Fig. 15 [Plate 224], an example (from an SRC J plate) of the former effect is shown; this is NGC 1411.

i) Photographic Artifacts

At very low contrast levels above the background, various kinds of emulsions exhibit correlations of different kinds among developed grains. As Ghigo (1978) has noted, fluctuations of this kind may produce spurious linear features at brightness levels near the plate limit, in a kind of "Martian canal" effect. For instance, most of the jet candidates listed by Vorontsov-Velyaminov (1966, 1972) appear, from inspection of Sky Survey plates, to have surface brightness too faint to be reliably detected from such material alone. Very faint features, unless they are quite large, must therefore be con-

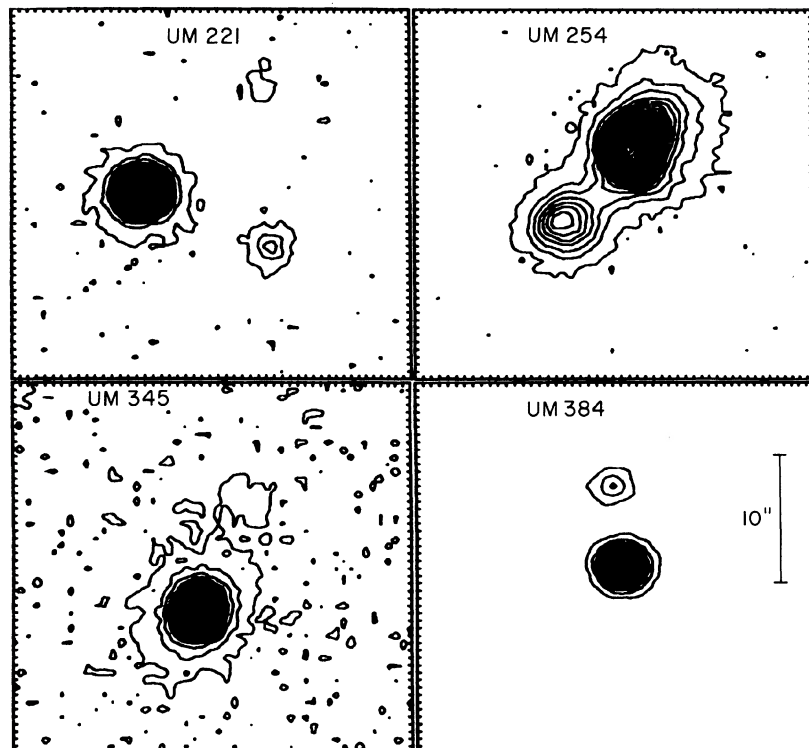


FIG. 14. Four Michigan-Tololo (UM) objects with reported jets; each is a companion galaxy or foreground star. Contour plots from CTIO 4 m CCD images in the blue.

firmed on deeper material. Some control over this effect may be exercised by noting the level at which tails not connected to anything start to appear on the plate.

The combination of a large (random) grain clumping and the steep exposure gradient of a galaxy envelope can be particularly eye-catching, and yield a very convincing jet image. This is well illustrated by UGC 1378 (Fig. 16, [Plate 225]). The red PSS image shows a jet in P.A. 160° , but deep images in B and R , and slit spectra, show nothing here. An M dwarf at $R \approx 21$ is present and may contribute part of the apparent feature. Similar features appear in sky-survey images of UGC 360 and 6435, but deep imaging and spectroscopy do not confirm their presence.

j) Galaxies with Chaotic Structures

Jets are obviously easiest to pick out against the smooth, regular background of an elliptical galaxy. In spirals of intermediate or late Hubble type, the internal structure can be so complex or disorganized that chance radial alignments of knots are not unlikely. There are clearly subjective tradeoffs to be made in selecting jet candidates among late-type galaxies. Clear hints to the possible presence of a jet are available when the feature extends outside the visible galactic structure or points to an active nucleus.

Irregular systems may exhibit jet-like structure, perhaps produced by propagating star formation. NGC 1602 is such a case (Sol 1983). The apparent jet consists of H II regions (Fig. 17, [Plate 226]), as does most of the rest of the galaxy, including the knot from which the jet issues. There is no evidence from these data that this feature is not an incidentally aligned set of H II regions relating only to the history of star formation in the galaxy, rather than to any mass motions or nuclear phenomena. Indeed, it is not clear that NGC 1602 has a distinct nucleus.

IV. CRITERIA FOR IDENTIFYING OPTICAL JETS

From the menagerie just reviewed, and photometric properties of galaxies with (generally accepted) jets from the literature or observed for this survey, several rules may be set up for finding optical jets on survey plates with a much smaller number of false alarms, albeit at the expense of some kinds of conceivable (but uncommon) jets.

(1) Genuine jets have no more than a few percent of the host galaxies' optical luminosity. Values for the luminosity ratio at B are collected in Table III for some objects generally accepted as ejected matter; in no case does the ratio exceed 0.03. By contrast, tidal features and superpositions approach a brightness ratio of unity, as in VV 144 (Keel 1985a) or III Zw 104 from the objects observed here. Objects with val-

TABLE III. Jet/galaxy brightness ratios, B band.

Galaxy	Ratio	Source
M87	0.005	de Vaucouleurs and Nieto 1979
PKS 0521-36	0.014	Keel 1985b
NGC 1097 (NE)	0.0011	CTIO CCD
3C 31	2.6×10^{-4}	Butcher, van Breugel, and Miley 1980
3C 66B	7.7×10^{-4}	Butcher, van Breugel, and Miley 1980
3C 273	0.025	Kron, Ables, and Hewitt 1972; Tyson, Baum, and Kreidl 1982
ESO 0610-23	0.005	CTIO CCD
NGC 1598 (S)	0.0025	CTIO CCD
ESO 2330-38	0.10	CTIO CCD
ESO 0304-47	0.07	CTIO CCD
AM 0207-49	0.44	CTIO CCD
VV 144	1.0	Keel 1985a

Notes to TABLE III

Nonthermal nuclear sources are not included in the galaxy light. Objects are grouped by probable nature: jets at the top, possible jets in the middle, and tidal features at the bottom.

ues of the ratio lower than about 10^{-3} are generally not found on Sky Survey plates. Objects with high values (~ 0.02) but jets that are short compared to a galaxy scale length may also be missed through overexposure of the inner part of the galaxy, as is the case with M87. This is the most obvious limitation of deep optical searches with photographic material.

(2) Jets are either one-sided or very asymmetric in optical intensity. The only radio galaxies in which emission of some sort is seen on both sides of the nucleus have at least one side associated with the extended lobes, rather than the jets themselves (e.g., van Breugel *et al.* 1985). Two pairs of opposing jets are seen in NGC 1097; Lorre (1978) gives the peak surface-brightness ratio of the pairs as 3:1 (N-S) and 9:1 (NE-SW). The CCD data obtained here suggest that 3:1 is an overestimate for the overall N-S intensity ratio. Edge-on polar rings and tidal features, on the other hand, frequently appear very symmetric in brightness and structure; many of them may be eliminated by this rule.

(3) One-sided extensions along the major axes of highly inclined galaxies are likely to be spiral arms (Fig. 11) and should be excluded from jet surveys.

(4) Careful comparison of the claimed feature with nearby blank sky must be done from survey plates, to see whether it is above the apparent intensity of the quasilinear clumpings usually shown by grain patterns. This is especially troublesome in extensive low-surface-brightness envelopes, in which the background light raises the local mean level and so makes such change fluctuations more apparent (Fig. 16).

(5) The jets so far observed optically are all quite straight and narrow. That of M87 is barely resolved in width at the $1''$ level (de Vaucouleurs and Niéto 1979), and that of PKS 0521-36 has a width so far resolved only at 2 cm (Keel 1985b). An aspect ratio of about 8:1 may be used to separate jets and other objects, when the available angular resolution is sufficient to make a measurement. Similarly, even though such features as the M87 jet show "wiggles," their amplitude over the optically detected region still falls within this aspect ratio. These criteria may be further quantified when more objects have been measured.

IV. THREE CANDIDATE JET GALAXIES

After weeding out the classes of objects just discussed, some jet candidates or ambiguous cases do remain among the galaxies observed here. This section describes three of these objects, and problems in their interpretation.

a) ESO 0610-23

This system appears elliptical-like on sky-survey plates, with a knotty jet at P.A. 41° . CCD images (Fig. 18(a), [Plate 227]) show that the galaxy possesses substantial nonaxisymmetric structure. After subtracting a version of the image smoothed with a $7''$ circular median filter (high-pass filtering), the blue image shows complex internal structure, including dust patches or lanes as well as a network of bright features [Fig. 18(b)]. A SIT spectrum along the jet shows H II region emission all along the galaxy, with $[\text{N II}]/\text{H}\alpha$ and $[\text{S II}]/[\text{N II}]$ indicative of low-metallicity gas (Rubin *et al.* 1984). A gray-scale display of the region near H α (Fig. 19, [Plate 228]) shows the very weak $[\text{N II}]$ throughout the system, and somewhat stronger $[\text{S II}]$.

The velocity structure traced by the emission lines shows a smooth, small-amplitude pattern with a few bright emission

regions at other velocities. The total range in velocity is slightly less than 150 km/s; any large-scale motions must be nearly in the plane of the sky.

Physical interpretation of this system remains ambiguous. The jet appears to extend in the direction of part of the inner structure [Fig. 18(b)], which might suggest some edge-on disk structure. Any rotation in the ionized gas, however, is of small amplitude (less than 90 km/s), perhaps not unusual for a galaxy of such low luminosity ($V \approx 14.0$, $M_V \approx -18$). The inner structure with a peak displaced from the center of the outer isophotes, dust patches, and spatially extensive star formation suggests a merger, but the jet is a single extension far out into the envelope with no counterpart elsewhere in the galaxy, and is not clearly connected with the inner structures. A high-resolution velocity map would be of great help in unraveling the history and present state of this system.

b) UGC 3995

This system of two spiral galaxies, which overlap in projection, is listed in the notes to the UGC as "double system, jets." The image-tube plate (Fig. 20(a), [Plate 229]) shows what may be either a faint jet or an extension of one of the arms of the fainter galaxy (UGC 3995 B). An H α image [Fig. 20(b)] shows H II regions along the arms of both galaxies, especially A, and strong nuclear emission in UGC 3995 A. This nucleus is, in fact, a Type 2 Seyfert, as seen in an IDS spectrum (Fig. 21).

Deeper images to confirm or deny the presence of a jet are most desirable. The presence of an active nucleus lends some credence to the idea of nuclear ejection, but the probability of seeing such a nucleus is enhanced in closely paired systems (e.g., Kennicutt and Keel 1984; Keel *et al.* 1985), so that the presence of a Seyfert may reflect an interaction which could also give rise to faint, asymmetric outer features. The companion UGC 3995 B shows a highly composite nuclear spectrum with Ca II H and K absorption and weak H α emission, with a projected velocity difference of 400 km/s.

c) NGC 1598

Hawarden *et al.* (1979) reported two opposed jet-like features in this galaxy, based on a contrast-enhanced IIIa-J UK Schmidt plate. To confirm the existence of these features and attempt to clarify their nature, CCD images of NGC 1598 were obtained with the CTIO 4 m. Since the features are much larger than either the seeing disk or the pixel size, spatial filtering could be used to improve their detectability above sky + readout noise. Gaussian smoothing (FWHM $5'' = 8.8$ pixels) was most successful, as shown in Fig. 22 [Plate 230]. The linear features are confirmed here, as are the faint external spiral arms continuing the inner pattern seen on the UKST plate. A feature more nearly tangential to the disk originating near the southeast jet is also seen, and appears at a lower relative contrast on the UKST plate. In fact, there is considerable irregular structure both northwest and southeast of the galaxy, between the inner disk and external arms. The different relative intensities of this structure and the jets on CCD and photographic images points up the importance of understanding the spatial-frequency properties of the analog or digital processes used to bring out faint features such as these. Many processes, including median windowing and its analog cousin unsharp copying, emphasize a specific range of frequencies most strongly, and can in fact sharpen the peak of a diffuse feature.

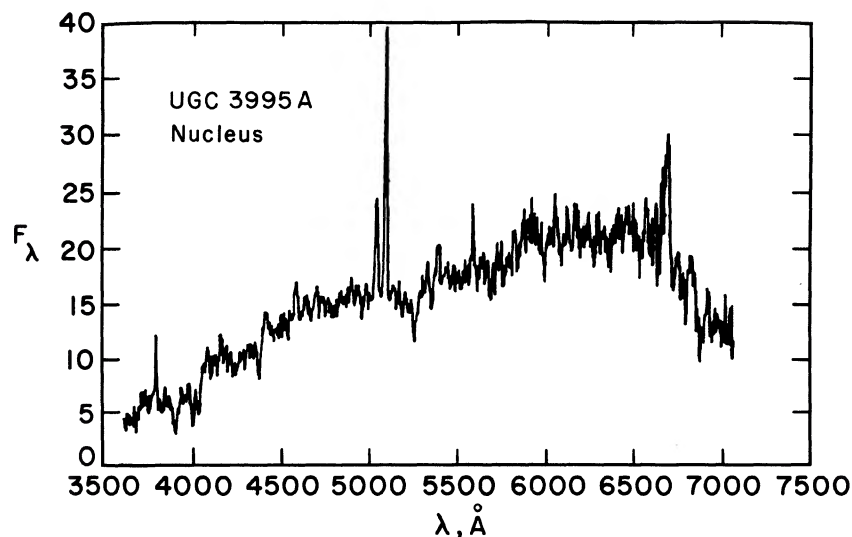


FIG. 21. Spectrum of the nucleus of UGC 3995 A, taken with the KPNO 2.1 m and IIDS, using 6.1" apertures. This is a Type 2 Seyfert, with very high $[O\ III]/H\beta$, but no strong nonstellar continuum.

The nucleus of NGC 1598 has been observed spectroscopically by Hawarden *et al.* (1979) and by Phillips *et al.* (1985); low-ionization emission is present, as in the suggested analog NGC 1097. The galaxy is in a small group with NGC 1595 and the Carafe galaxy; part of the envelope of NGC 1595 (an elliptical) appears at the edge of Fig. 22. Once again, the effects of interactions and nuclear activity are difficult to distinguish, since the "chaotic" matter and apparent jets might represent a tidal disturbance due to NGC 1595, or its aftermath.

V. CONCLUSIONS

A number of galaxies previously suggested to contain optical jets have been surveyed with imaging and spectroscopy. Most may be shown to be examples of tidal effects, superpositions, illusions due to optical-depth effects in edge-on galaxies, or photographic artifacts. For these objects, the results are listed here to guide further work on these systems into appropriate channels.

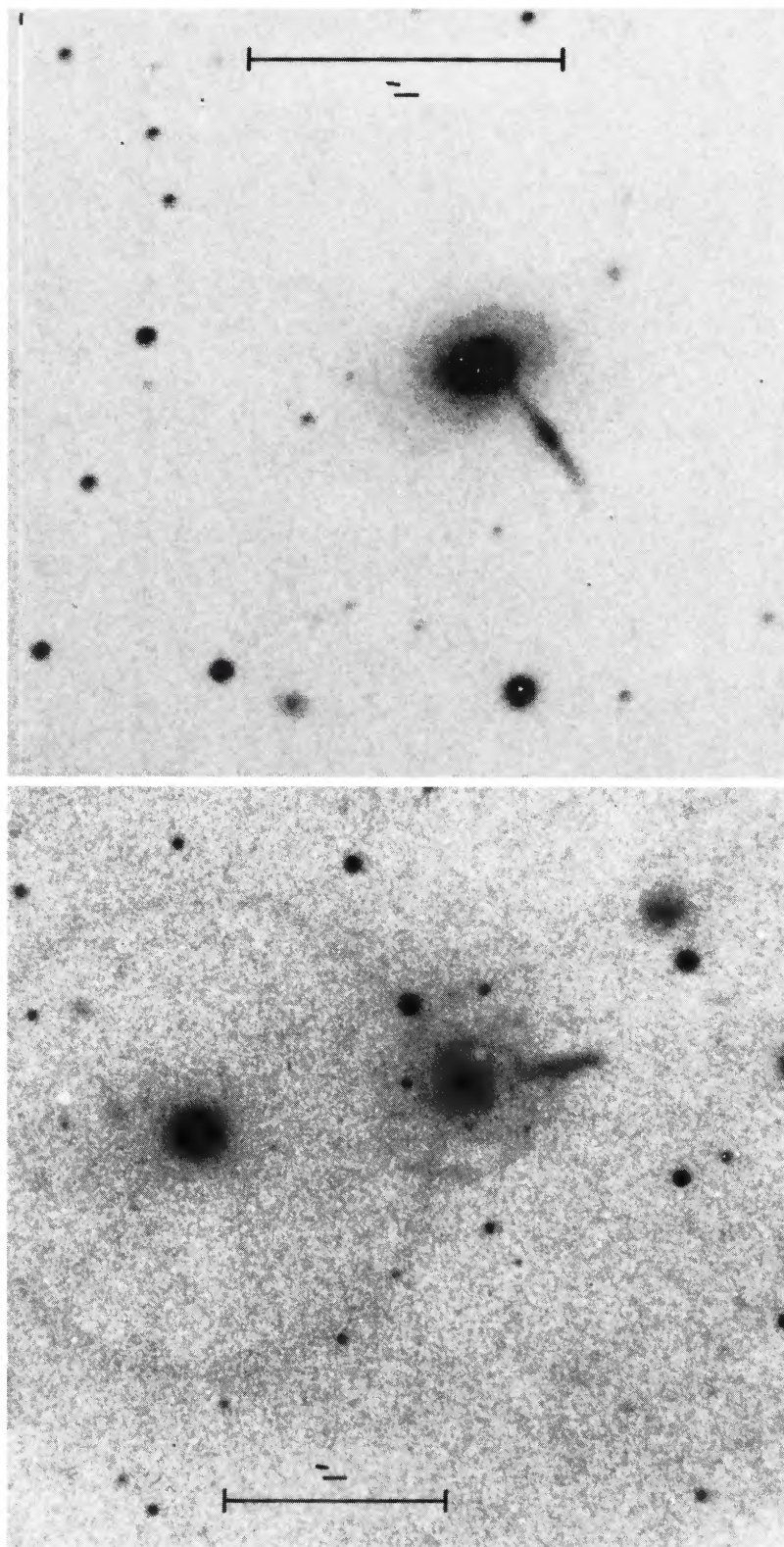
A few systems do show evidence of features that might be jets, in the sense of having been ejected from the nucleus. These are worthy of closer examination, as described in Sec. IV. From the properties of all the systems of each kind observed in this study, a set of rules useful in separating them morphologically on Sky Survey plates is proposed. These have been listed in the hope that the study of jets in the optical may be less confused by interesting but irrelevant objects than has occasionally been the case.

I am grateful for discussions with Drs. N. Sharp and H. Arp, and for additional objects brought to my attention by H. Sol and E. Sadler. Dr. Arp made his 5 m plates available for measurement and arranged for my use of the measuring equipment in Pasadena. The observations at Mount Lemmon were supported by the NSF through operating grants to UCSD.

REFERENCES

- Arp, H. C. (1967). *Astrophys. Lett.* **1**, 1.
 Arp, H. C., and Madore, B. F. (1977). *Mon. Not. R. Astron. Soc.* **18**, 234.
 Balick, B., and Heckman, T. M. (1981). *Astron. Astrophys.* **96**, 271.
 Bertola, F., and Sharp, N. A. (1984). *Mon. Not. R. Astron. Soc.* **207**, 47.
 Biretta, J. A., Owen, F. N., and Hardee, P. E. (1983). *Astrophys. J. Lett.* **274**, L 27.
 Butcher, H. R., van Breugel, W. J. M., and Miley, G. K. (1980). *Astrophys. J.* **235**, 749.
 de Vaucouleurs, G. (1958). *Astrophys. J.* **127**, 487.
 de Vaucouleurs, G., and Niéto, J.-L. (1979). *Astrophys. J.* **231**, 364.
 Ford, H. C., and Butcher, H. R. (1977). *Astrophys. J. Suppl.* **41**, 147.
 Fricke, K. J., Kollatschny, W., and Loose, H.-H. (1984). *Nature* **309**, 600.
 Ghigo, F. D. (1978). *Astron. J.* **83**, 1363.
 Graham, J. A. (1982). *Publ. Astron. Soc. Pac.* **94**, 244.
 Hawarden, T. G., Longmore, A. J., Cannon, R. D., and Allen, D. A. (1979). *Mon. Not. R. Astron. Soc.* **186**, 495.
 Heckman, T. M. (1981). *Astrophys. J. Lett.* **250**, L59.
 Keel, W. C. (1984). *Astrophys. J.* **279**, 550.
 Keel, W. C. (1985a). *Astron. J.* **90**, 1449.
 Keel, W. C. (1985b). *Astrophys. J.* (in press).
 Keel, W. C. (1985c). In preparation.
 Keel, W. C. (1985d). *Astrophys. J.* (submitted).
 Keel, W. C., Kennicutt, R. C., Jr., Hummel, E., and van der Hulst, J. M. (1985). *Astron. J.* **90**, 708.
 Kennicutt, R. C., Jr., and Keel, W. C. (1984). *Astrophys. J. Lett.* **279**, L5.
 Kron, G. E., Ables, H. D., and Hewitt, A. V. (1972). *Publ. Astron. Soc. Pac.* **84**, 303.
 Lauberts, A. (1982). *ESO/Uppsala Survey of the ESO(B) Atlas* (ESO, Munich).
 Laustsen, S., and West, R. M. (1980). *J. Astron. Astrophys.* **1**, 177.
 Lorre, J. (1978). *Astrophys. J. Lett.* **222**, L99.
 MacAlpine, G. M., Lewis, D. W., and Smith, S. B. (1977). *Astrophys. J. Suppl.* **35**, 302.
 MacAlpine, G. M., and Lewis, D. W. (1978). *Astrophys. J. Suppl.* **36**, 587.
 Malin, D. F. (1979). *Nature* **277**, 279.
 Malin, D. F., and Murdin, P. (1984). *Colours of the Stars* (Cambridge University, Cambridge), p. 59.
 Miley, G. K., Heckman, T. M., Butcher, H. R., and van Breugel, W. J. M. (1981). *Astrophys. J. Lett.* **277**, L5.
 Mould, J., Balick, B., Bothun, G., and Aaronson, M. (1982). *Astrophys. J. Lett.* **260**, L37.
 Nieto, J.-L., and Lelièvre, G. (1982). *Astron. Astrophys.* **109**, 95.
 Nilson, P. (1973). *Uppsala General Catalog of Galaxies* (Uppsala University, Uppsala).

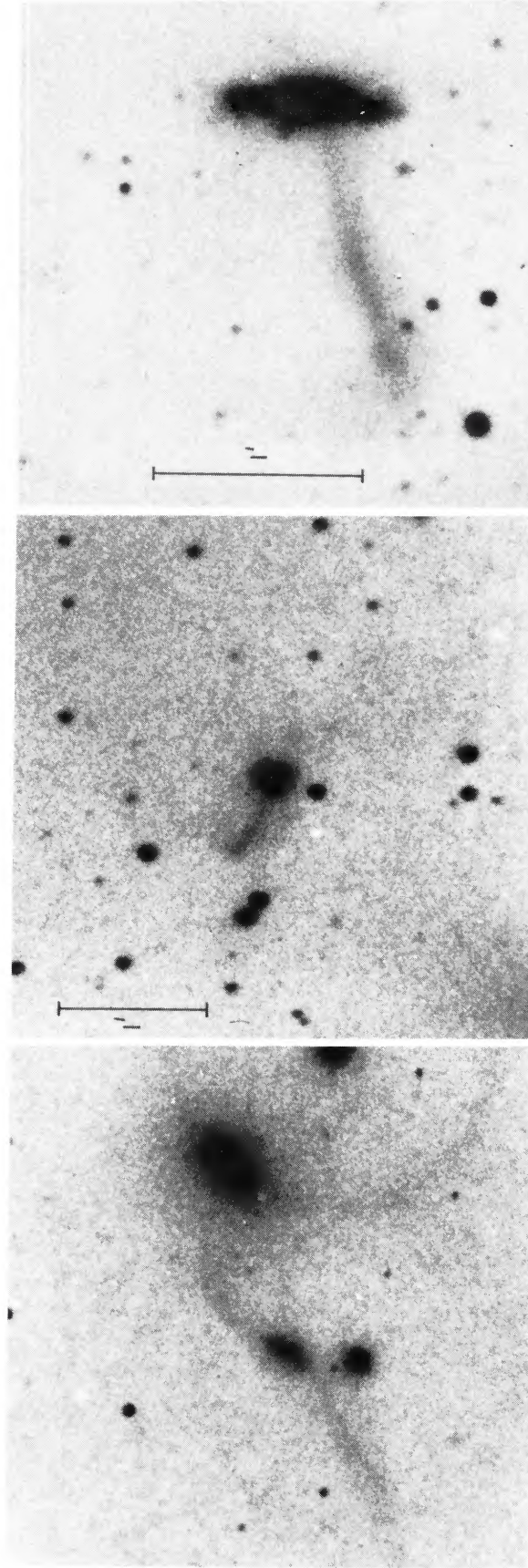
- Owen, F. N., Eilek, J. A., O'Dea, C., Inoue, M., and White, R. A. (1985). *Bull. Am. Astron. Soc.* **16**, 882.
- Phillips, M. M., Pagel, B. E. J., Edmunds, M. G., and Díaz, A. (1985). Preprint.
- Romanishin, W. (1984). *Publ. Astron. Soc. Pac.* **96**, 24.
- Rubin, V. C., Ford, W. K., Jr., and Whitmore, B. C. (1984). *Astrophys. J. Lett.* **281**, L21.
- Schweizer, F., Whitmore, B. C., and Rubin, V. C. (1983). *Astron. J.* **88**, 909.
- Simkin, S. M., Bicknell, G. V., and Bosma, A. (1984). *Astrophys. J.* **277**, 513.
- Simkin, S. M., and Ekers, R. D. (1979). *Astron. J.* **84**, 56.
- Sofue, Y., Fukui, Y., Fujimoto, M., Deguchi, S., and Wakamatsu, K. (1982). *Astron. J.* **87**, 980.
- Sol, H. (1983). *ESO Messenger* **32**, 33.
- Stockton, A. (1972). *Astrophys. J.* **173**, 247.
- Stone, R. P. S. (1974). *Astrophys. J.* **193**, 135.
- Stone, R. P. S. (1977). *Astrophys. J.* **218**, 767.
- Sulentic, J. A., Arp, H. C., and Lorre, J. (1979). *Astrophys. J.* **233**, 44.
- Tsitsin, F. A. (1955). *Astron. Tsirk.* **157**, 10.
- Tyson, J. A., Baum, W. A., and Kreidl, T. (1982). *Astrophys. J. Lett.* **257**, L1.
- van Breugel, W. J. M., Heckman, T. M., Bridle, A., Butcher, H., Strom, R., and Balick, B. (1983). *Astrophys. J.* **275**, 61.
- van Breugel, W. J. M., Miley, G. K., Heckman, T., Butcher, H., and Bridle, A. (1985). *Astrophys. J.* **290**, 496.
- Vorontsov-Velyaminov, B. A. (1959). *Atlas and Catalog of Interacting Galaxies* (Shternberg Institute, Moscow).
- Vorontsov-Velyaminov, B. A. (1966). *Atti del Convegno Sulla Cosmologia* (Barbera, Firenze), p. 48.
- Vorontsov-Velyaminov, B. A. (1972). *Vnegalakticheskaia Astronomia (Extragalactic Astronomy)* (Nauka, Moscow), p. 329.
- Vorontsov-Velyaminov, B. A. (1977). *Astron. Astrophys. Suppl.* **28**, 1.
- Wolstencroft, R. D., Tully, R. B., and Perley, R. A. (1984). *Mon. Not. R. Astron. Soc.* **207**, 889.
- Zwicky, F. (1971). *Catalog of Selected Compact Galaxies and of Post-Eruptive Galaxies* (Speich, Zürich).



UGC 3810 B ESO 0534-52 V

FIG. 1. Superpositions of galaxies resembling jets. Left, UGC 3810, from a blue-light 2.1 m image-tube plate. Right, ESO 0534-52, from a 5 min V image with the CTIO 4 m and RCA CCD.

W. C. Keel (see page 2210)



NGC 1568 = II Zw 10 B IV Zw 120 B ESO 2330-38 V

FIG. 2. Galaxies with tidal tails cataloged as jets. Left, NGC 1568 = II Zw 10; from a blue 2.1 m image-tube plate; note the symmetric curving tails. Center, IV Zw 120, from a similar plate; note the resolved width and curvature of the tail. Right, ESO 2330-38, 20 min exposure with RCA CCD and V filter, CTIO 4 m. Note the width of the tail and its offset from the nucleus.

W. C. Keel (see page 2210)

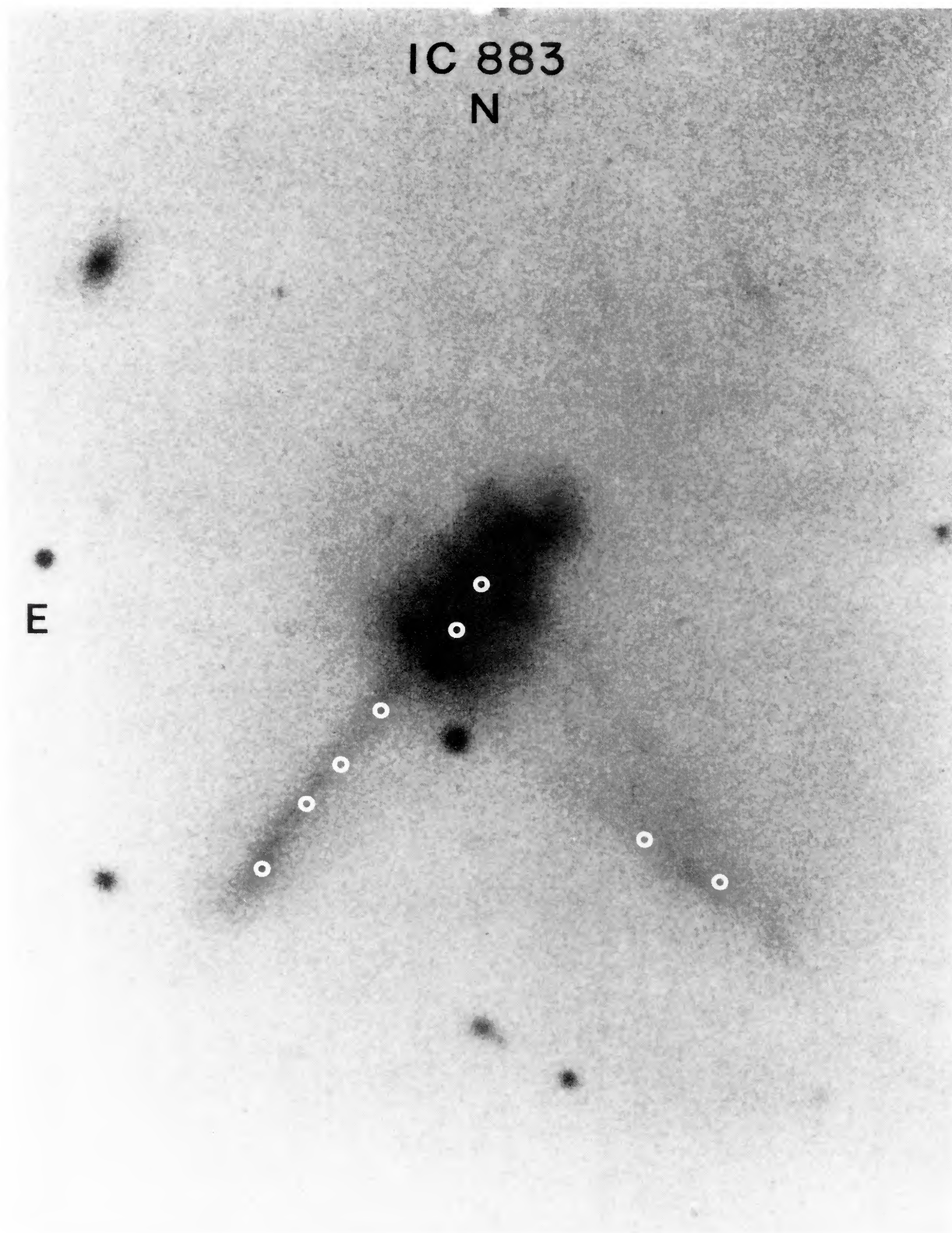


FIG. 4. IC 883, from the Arp (1966) atlas, with positions observed spectroscopically marked with circles to scale. Apertures of 2.5" diameter were used.

W. C. Keel (see page 2211)

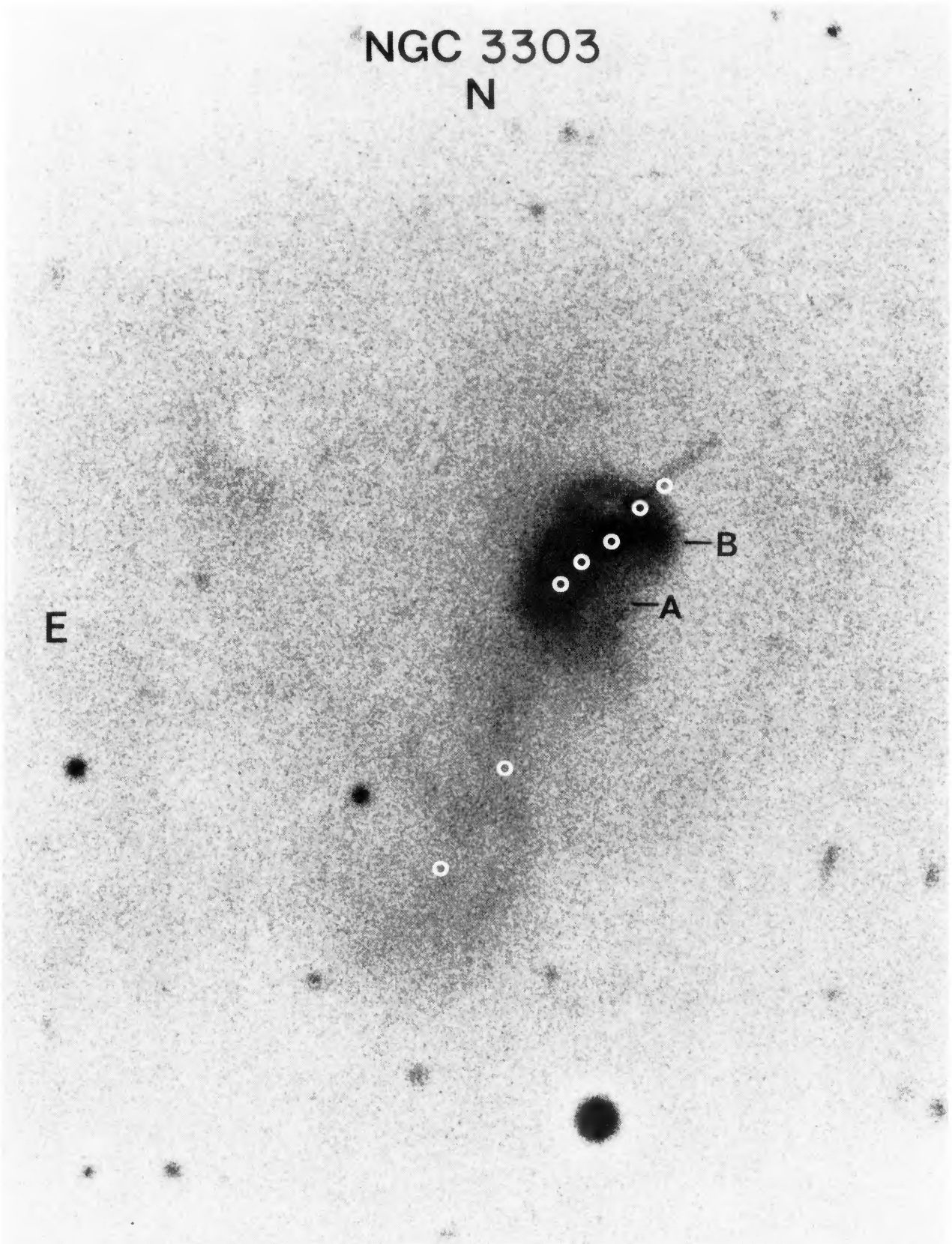
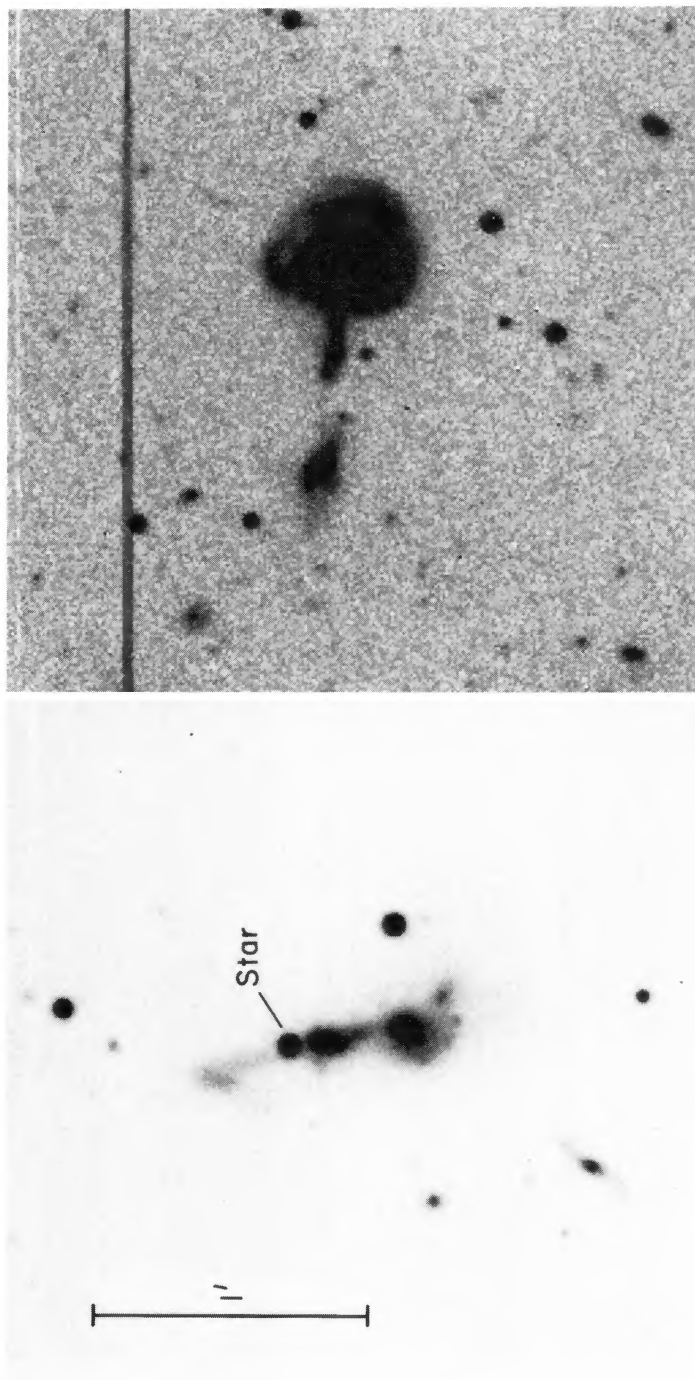


FIG. 6. NGC 3303, reproduced from the Arp atlas. Positions observed with the Cryogenic Camera are marked with circles of the correct size; the apertures were 2.5" in diameter.

W. C. Keel (see page 2211)

© American Astronomical Society • Provided by the NASA Astrophysics Data System



ESO 0304-47 V

AM 0207-49 V

FIG. 8. Further tidal features cataloged as jets. Left, AM 0207-49. Right, ESO 0304-47. Both are from 5 min *V* exposures with the CTIO 4 m and CCD.
W. C. Keel (see page 2211)

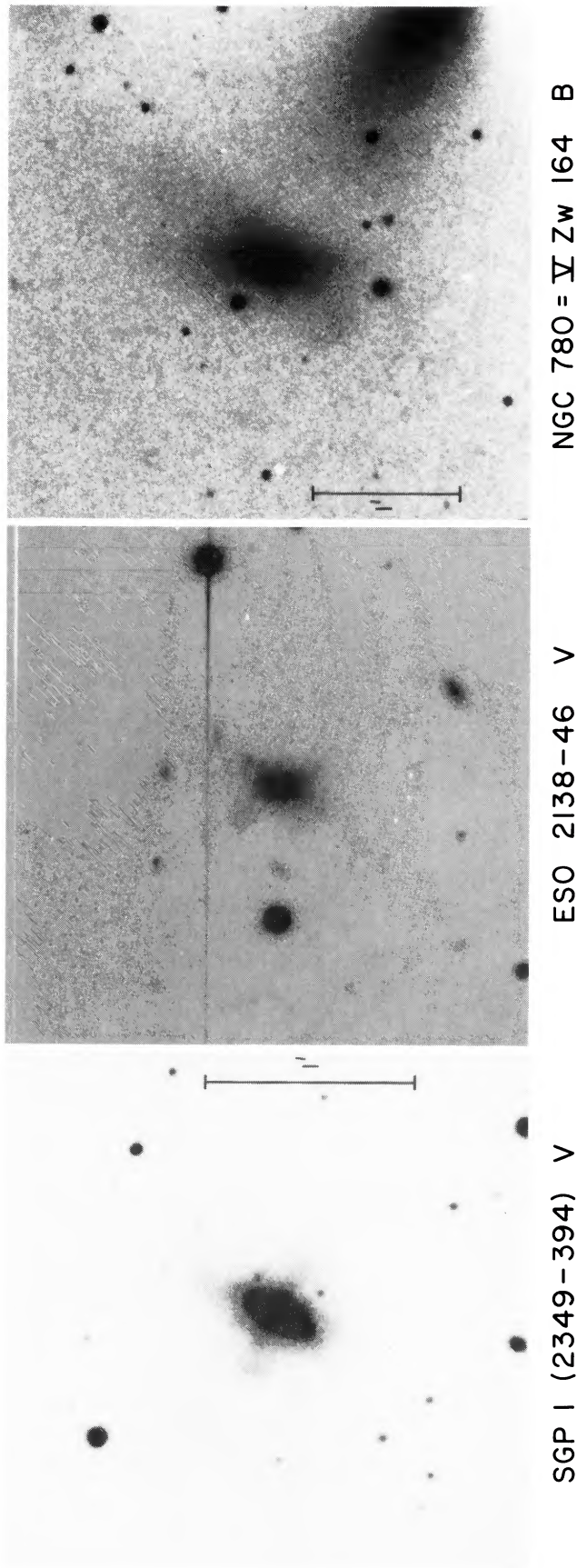


FIG. 10. Galaxies with polar or oblique rings found among cataloged jets. Left, SGP 1 (from the south Galactic pole region surveyed on SRCJ plates). Middle, ESO 2138-46 (both from 5 min CTIOCCD frames). Right, NGC 780 = UGC 1488 = V Zw 164, showing an oblique ring or outer disk (2.1 m blue image-tube plate).

W. C. Keel (see page 2212)

UGC 5050 = ARP 207

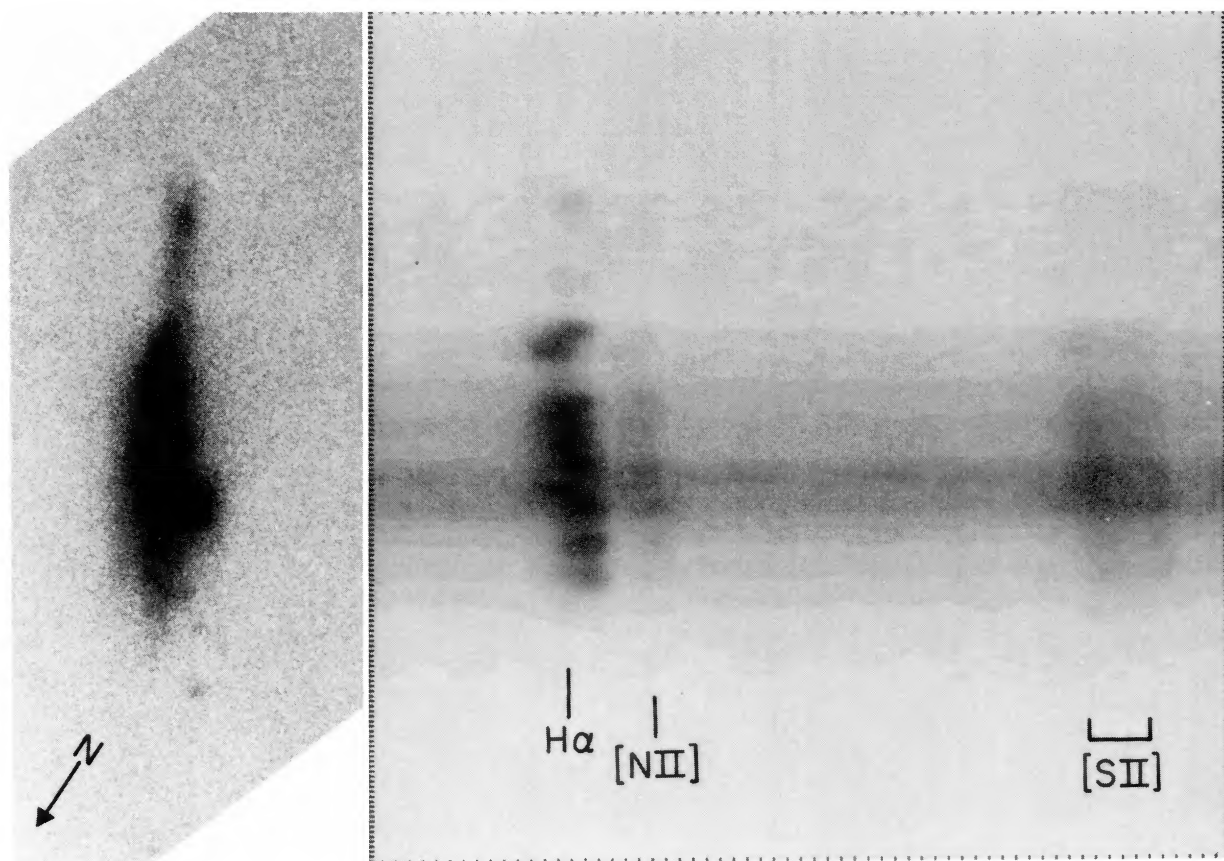


FIG. 11. UGC 5050 = Arp 207. The direct image is reproduced from the Arp atlas, and is oriented to match the accompanying Cryogenic Camera spectrum. The structure in $H\alpha$ emission indicates an imperfectly transparent disk seen edge-on, with discrete radial zones (arms) containing the $H\text{ II}$ regions. The jet at the top is thus the outside of a spiral arm whose counterpart on the other side is unseen due to the dust along its inner edge.

W. C. Keel (see page 2213)

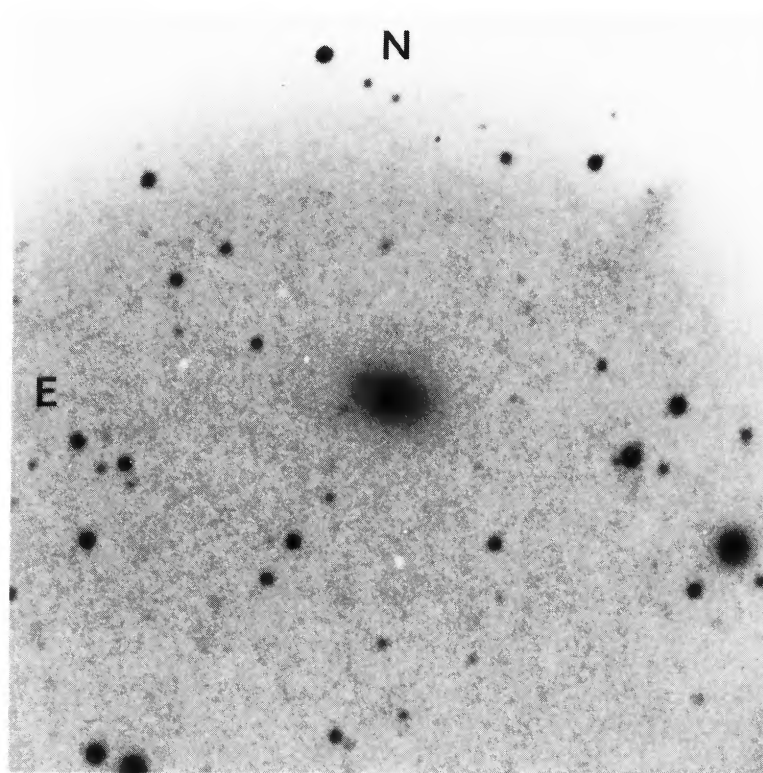
VII Zw 3 R

FIG. 12. VII Zw 3, a galaxy whose reported jet seems to be a bar in a faint disk (2.1 m red image-tube plate).

W. C. Keel (see page 2213)

NGC 573 = UGC 1078

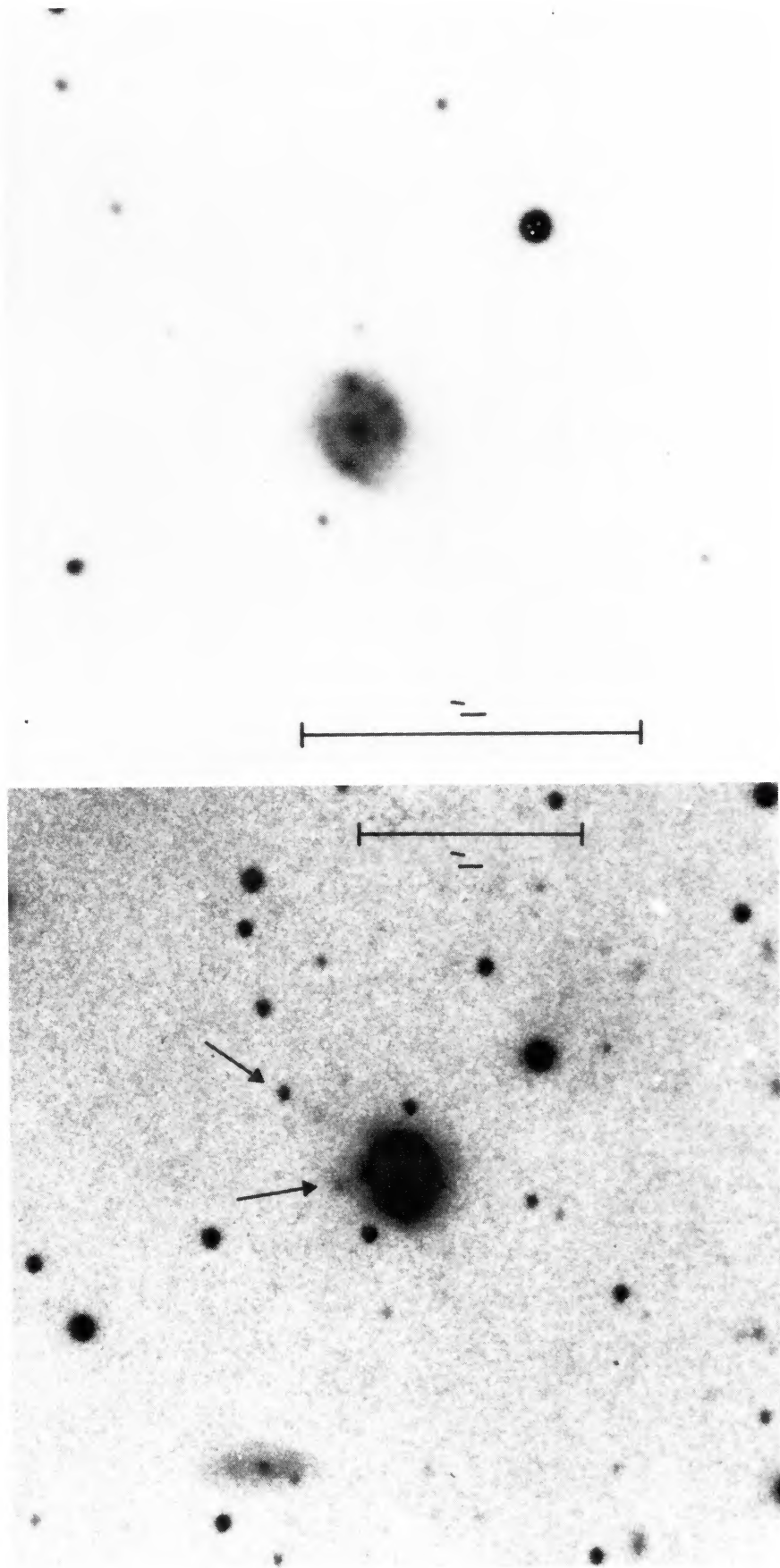


IMAGE - TUBE DIRECT B VIDEO CAMERA B

FIG. 13. "Stem" galaxy NGC 573 = UGC 1078. The outer regions and extended structures (arrowed) are shown in the blue image-tube plate (left); the inner regions and spiral structure appear in the blue video-camera frame at right.

W. C. Keel (see page 2213)

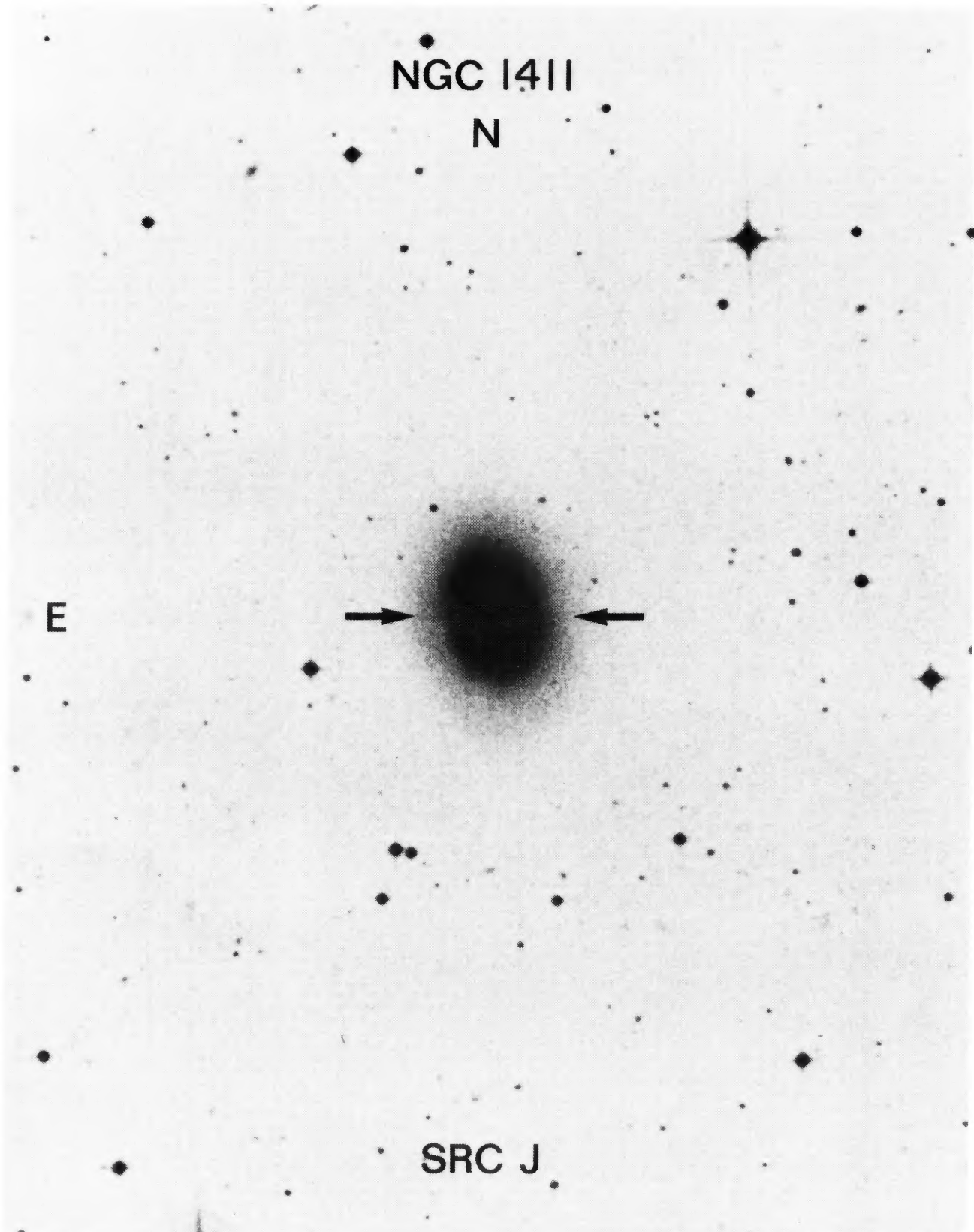
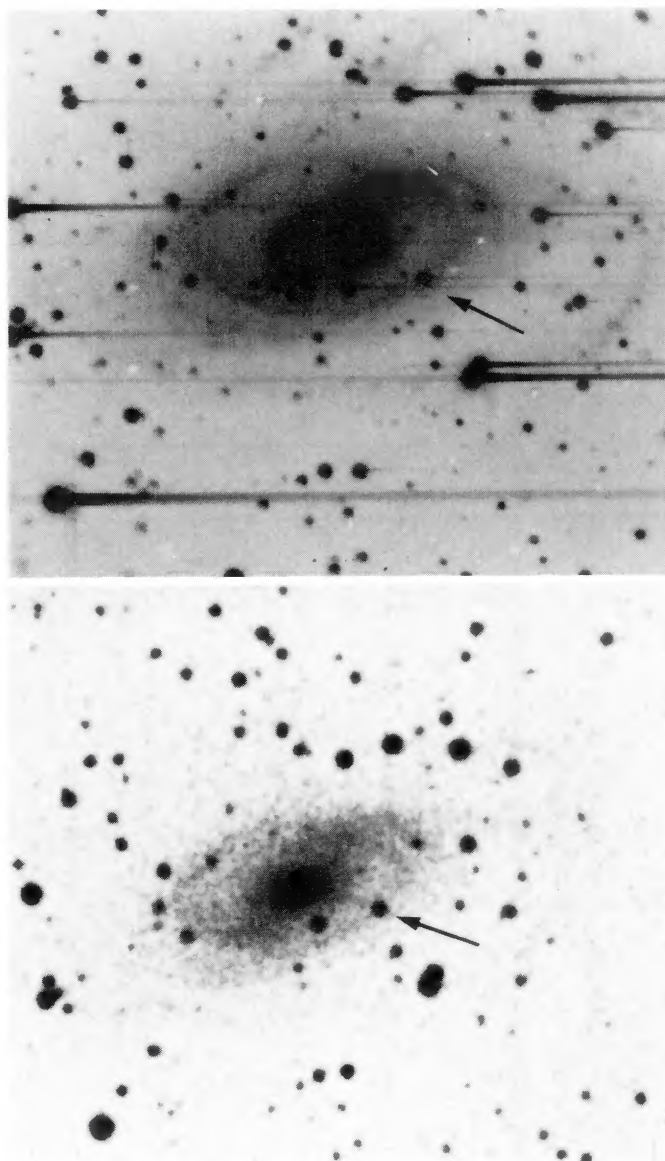


FIG. 15. Elliptical galaxy NGC 1411, from the SRC J survey, showing diffraction spikes from a projected foreground star. Such superpositions can mimic jets on material this deep.

W. C. Keel (see page 2213)

© American Astronomical Society • Provided by the NASA Astrophysics Data System

UGC 1378

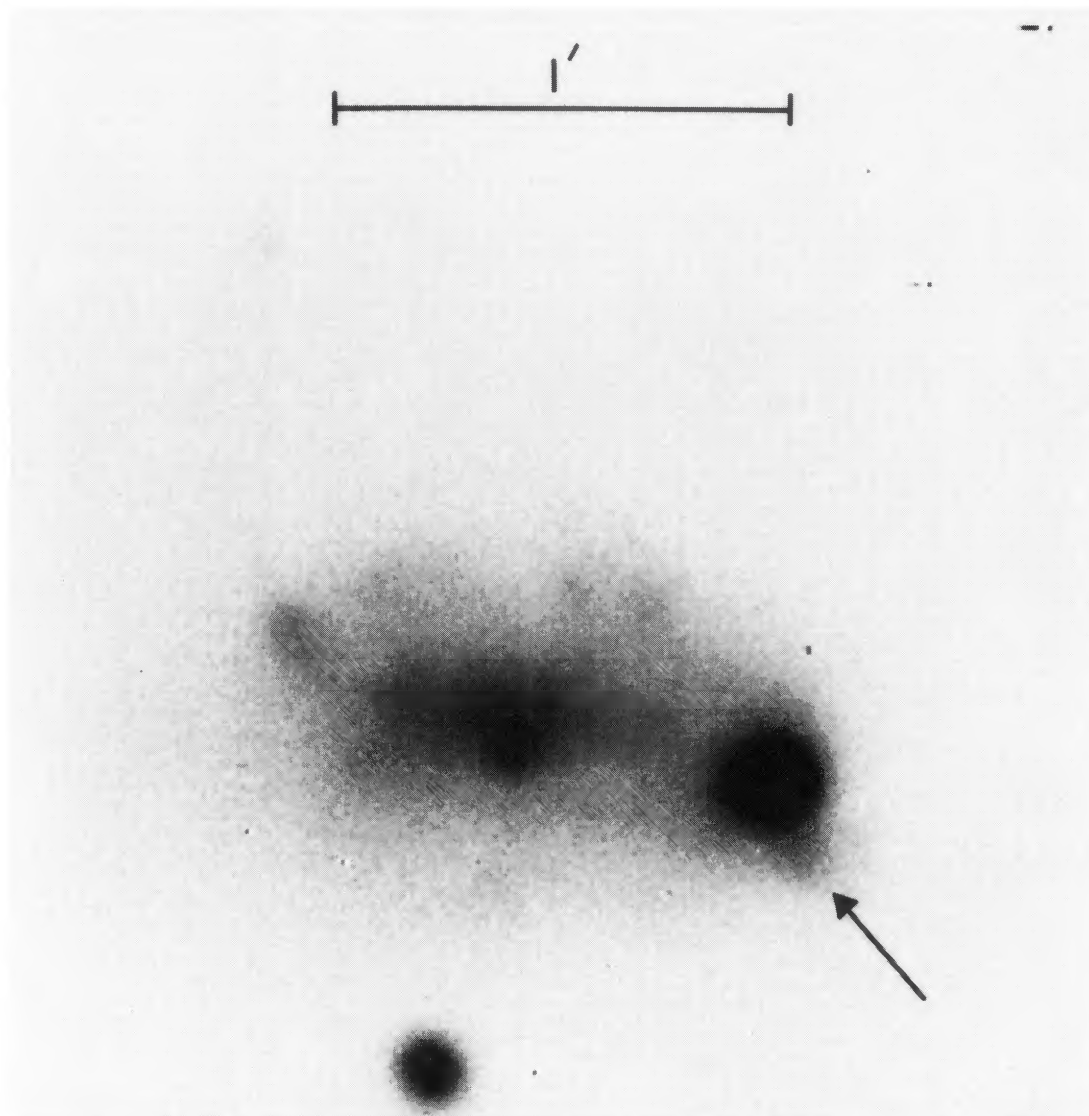


PSS E

CCD R

FIG. 16. Apparent jet of UGC 1378. Left, image from the PSS red plate; a jet-like feature emerges at P.A. 160°. Right, Cryogenic Camera direct image in *R*. The jet is not real, and appears to result from grain distribution plus a faint red star.

W. C. Keel (see page 2214)



NGC 1602 B

FIG. 17. Irregular galaxy NGC 1602, from a CTIO 4 m *B* CCD frame taken in poor seeing. The apparent jet from the brightest knot (arrowed) is a chain of H II regions.

W. C. Keel (see page 2214)

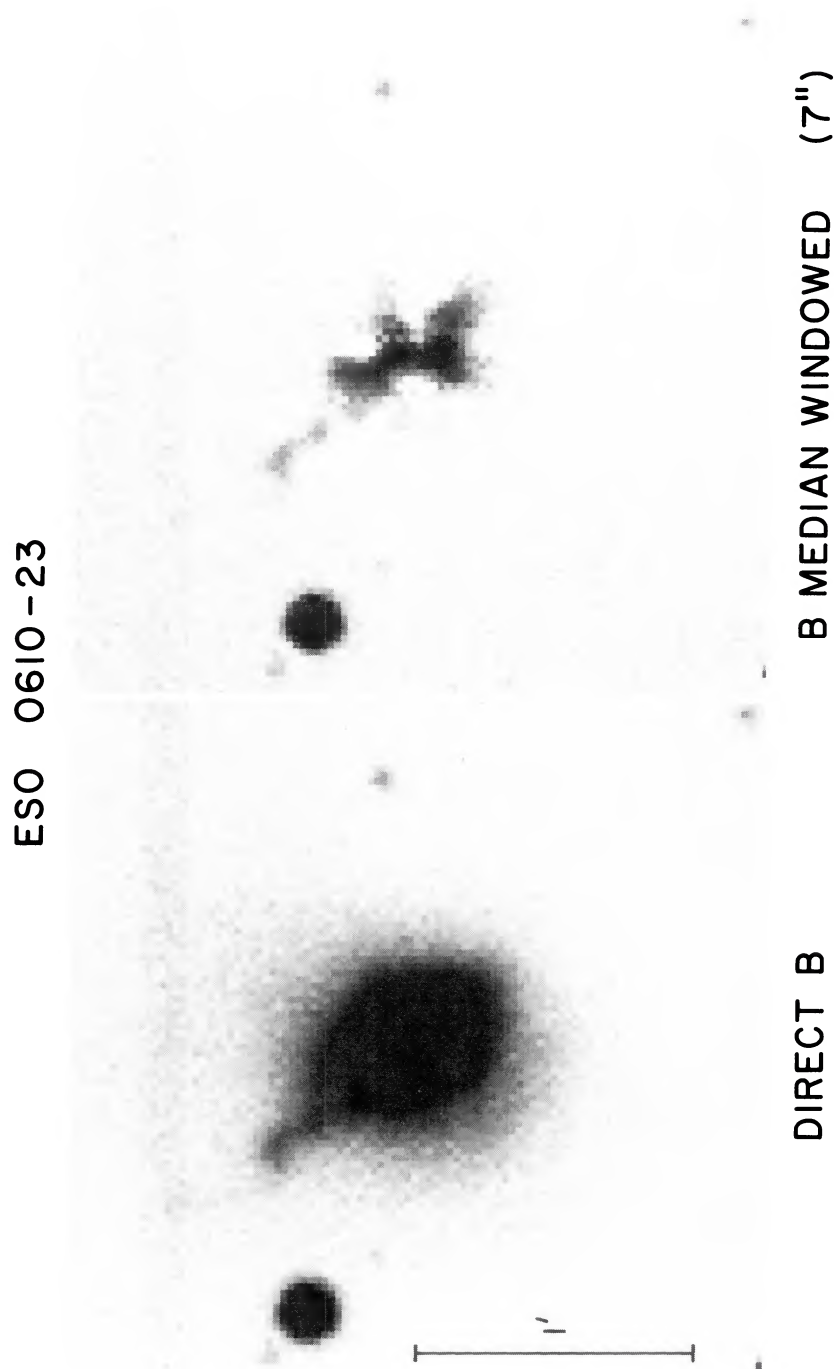


FIG. 18. Jet and internal structure of ESO 0610-23. Left, the original *B*-band CCD image, showing the knotty extension (jet?) to the northwest. Right, the same image enhanced to show detail on scales smaller than about 5" by subtracting a median-filtered version of the image, constructed using a circular window of 7" diameter. Complex structure and an off-center peak appear.

W. C. Keel (see page 2215)

ESO 0610-23 PA 41°

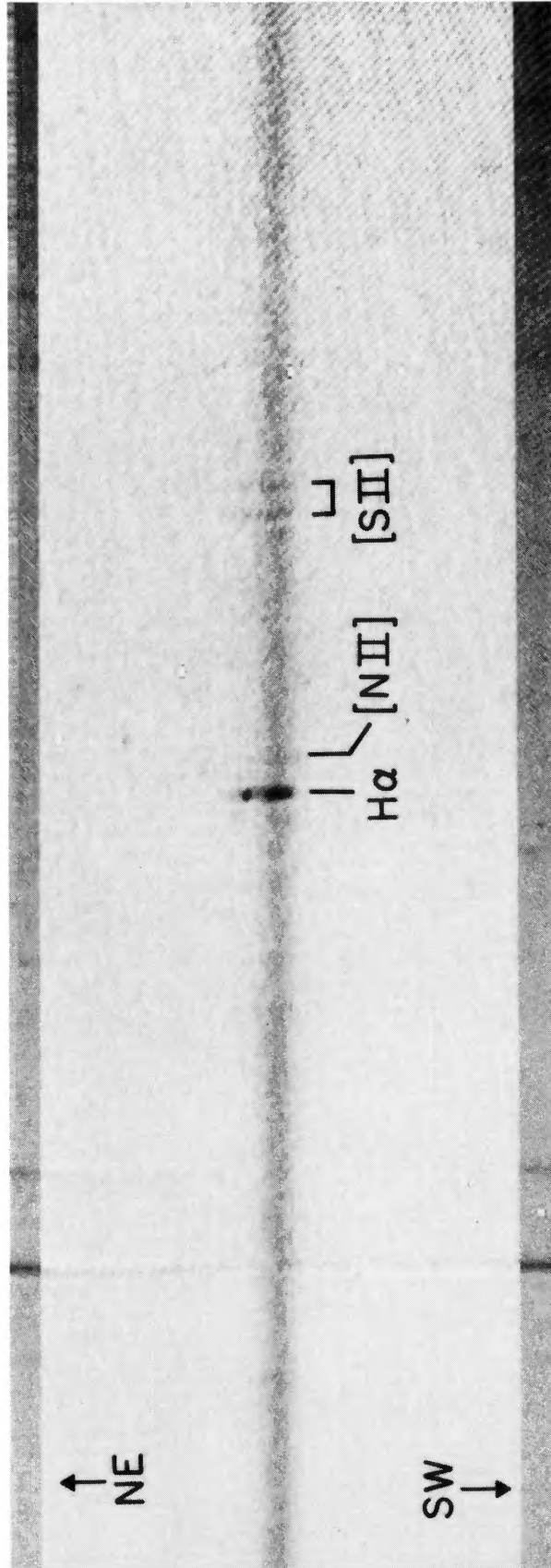
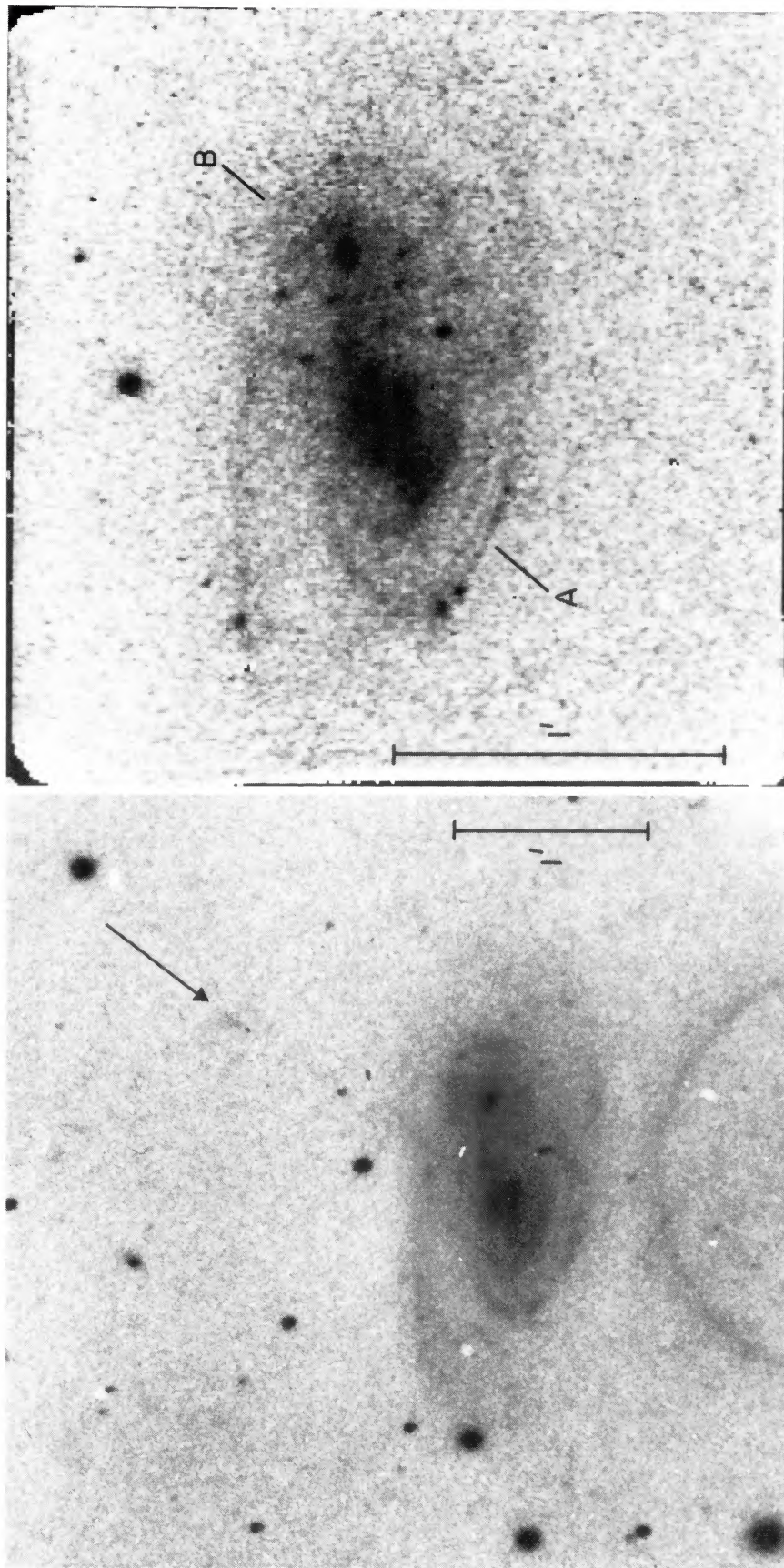


FIG. 19. SIT-Vidicon spectrum of ESO 0610-23 in the H α region. Taken in P.A. 141°, the spectrum shows H II region-like line ratios across the galaxy, including the apparent jet (top). The very low [N II]/H α and [N II]/[S II] ratios indicate low metallicity (Rubin, Ford, and Whitmore 1984).

W. C. Keel (see page 2215)

UGC 3995



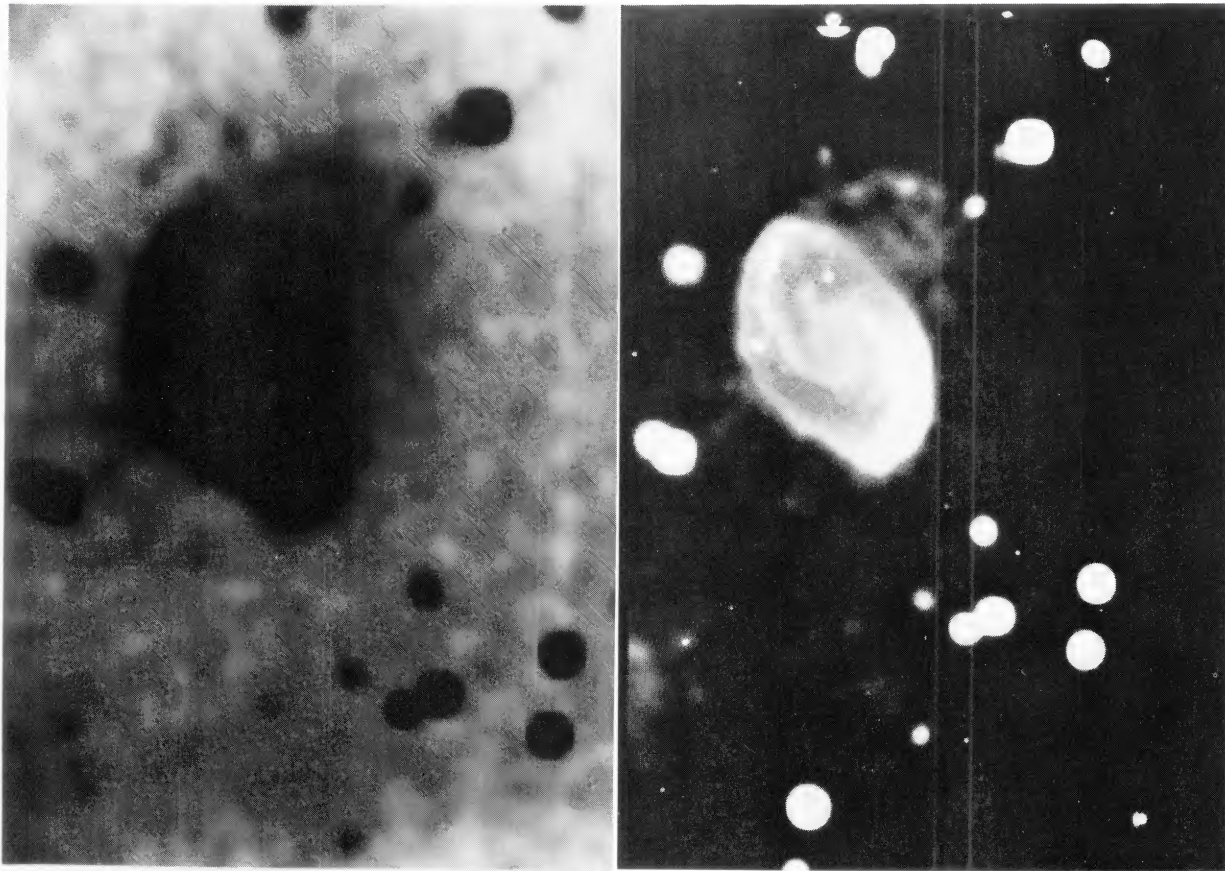
$\lambda 6650$

B

FIG. 20. Double system UGC 3995, with a jet or plume. Left, a broadband blue image-tube photograph, the jet extends toward the arrow. Right, a video-camera image through a filter 75 Å wide including redshifted H α .

W. C. Keel (see page 2215)

NGC 1598 V



5" GAUSSIAN

WITH ORIGINAL IMAGE

FIG. 22. Jets and extended structure of NGC 1598. Left, 5 min V CCD frame smoothed with a Gaussian of 5" FWHM, displayed to emphasize the faintest features. The reported jets appear to the NW and SE along with considerable structure in the outer parts of the galaxy. Right, the smoothed frame with the original image superimposed at lower contrast to show the relation between the inner arms and outer structure. Part of the elliptical galaxy NGC 1595 appears to the lower left; interaction with this galaxy may be responsible for some of the features in NGC 1598. Unlike the other figures in this paper, this one has north at the left and east at the top.

W.C. Keel (see page 2215)